Bub3-Bub1 binding to Spc7 (KNL1) toggles the spindle checkpoint switch by licensing interaction of Bub1 with Mad1-Mad2

Maria del Mar Mora-Santos[1], America Hervas-Aguilar[1], Katharina Sewart[2], Theresa C. Lancaster[1], John C. Meadows[1,3] and Jonathan B.A. Millar[1,4]

1 Division of Biomedical Sciences, Warwick Medical School, University of Warwick, Gibbet Hill, Coventry, CV4 7AL, UK

2 Department of Biological Sciences and Biocomplexity Institute, Virginia Tech, Blacksburg, VA 24061, USA

3 Institute of Advanced Study, University of Warwick, Gibbet Hill, Coventry, CV4 7AL, UK

4 Corresponding author

Email: J.Millar@warwick.ac.uk

Phone: 02476150414

FAX: 02476523568

Summary

The spindle assembly checkpoint (SAC) ensures that sister chromatids do not separate until all chromosomes are attached to spindle microtubules and bi-oriented. Spindle checkpoint proteins, including Mad1, Mad2, Mad3 (BubR1), Bub1, Bub3 and Mph1 (Mps1) are recruited to unattached and/or tensionless kinetochores. SAC activation catalyses the conversion of soluble Mad2 (O-Mad2) into a form (C-Mad2) that binds Cdc20, BubR1 and Bub3 to form the mitotic checkpoint complex (MCC), a potent inhibitor of the anaphase promoting complex (APC/C). SAC silencing de-represses Cdc20-APC/C activity allowing poly-ubiquitination of Securin and Cyclin B, leading to the dissolution of sister chromatids and anaphase onset [1]. Understanding how microtubule interaction at kinetochores influences the timing of anaphase requires an understanding of how spindle checkpoint protein interaction with the kinetochore influences spindle checkpoint signalling. We, and others, recently showed that Mph1 (Mps1) phosphorylates multiple conserved MELT motifs in the Spc7 (Spc105 / KNL1) protein to recruit Bub1, Bub3 and Mad3 (BubR1) to kinetochores [2-4]. In budding yeast, Mps1 phosphorylation of a central non-catalytic region of Bub1 promotes its association with the Mad1-Mad2 complex, although this association has not yet been detected in other organisms [5]. Here we report that multisite binding of Bub3 to the Spc7 MELT array toggles the spindle checkpoint switch by permitting Mph1 (Mps1) dependent interaction of Bub1 with Mad1-Mad2.

Results and Discussion

Bub3-Bub1 binding to Spc7 MELT motifs toggles the spindle checkpoint switch

The N-terminus of the fission yeast KNL1 homologue, Spc7, contains 12 MELT motifs that can be phosphorylated by Mph1 (Mps1) kinase *in vitro* [3, 4]. To examine the role of MELT motifs in controlling Bub1 binding and checkpoint signalling we created a sequence of mutants, *spc7-12TA*, *spc7-9TA*, *spc7-7TA*, *spc7-5TA*, *spc7-3TA* or *spc7-1TA*, in which some or all of the threonine and serine residues in these motifs were mutated to non-phosphorylatable alanine (Figure S1A). Binding of Bub1 to kinetochores was assayed in these mutants by quantitative fluorescence microscopy in cells that were arrested in mitosis by overexpression of Mad2. This revealed a wide dynamic range of Bub1 binding to kinetochores in individual cells and, as the number of phosphorylatable MELT sites was reduced, progressively lower average binding to kinetochores and inversely higher levels of nucleoplasmic Bub1 (Figures 1A & S1B-C), while the total Bub1 abundance stayed constant (Figure S1E). In parallel, we measured the ability of individual *spc7-mutant* cells, bearing a cold sensitive allele of β-tubulin (*nda3-KM311*) and a marker for high Cdk1 activity (Plo1-GFP), to mount a spindle checkpoint arrest. Whilst most *spc7-1TA*, *spc7-3TA*, *spc7-5TA* and *spc7-7TA* cells fully arrested, *spc7-9TA* and *spc7-12TA* cells mounted only a partial checkpoint response compared to wild type cells (Figure 1B & S1C-D). Similar results were observed in population studies of synchronised *nda3-KM311 spc7-mutant* cells, which express a marker that only appears in anaphase (Nsk1-GFP). Whilst a partial checkpoint response was still mounted in *spc7-7TA* cells, *spc7-9TA* and *spc7-12TA* cells were largely defective (Figure 1C & S1G). We note that the checkpoint in *spc7-12TA* cells is not as defective as in cells lacking *mad3*, suggesting that the SAC can be partially activated in this mutant (Figures 1B-C).

Spindle checkpoint protein homeostasis is crucial for the robustness of the checkpoint response in that even minor changes in the protein concentration of Mad1, Mad2, Mad3 and Cdc20 alter the threshold at which cells are able to delay anaphase onset in response to unattached kinetochores [6]. To examine whether the switch-like spindle checkpoint response from the Spc7-MELT array is sensitive to changes in Bub1 and Bub3 levels, we altered the expression of these proteins in a mutant defective in their kinetochore binding. Deletion of Bub3 strongly suppressed the checkpoint deficiency in *spc7-12TA* cells, as previously observed (Figure 1D & S1H, [4]). This

effect is not due to up-regulation of Bub1 protein levels (Figure S1F). Conversely, expression of an extra copy of Bub1 also strongly suppressed the checkpoint deficiency of *spc7-12TA* cells, whereas expression of an extra copy of Bub3 had no effect (Figure 1D). We conjecture that the inability of cells to mount a checkpoint response, when Bub3-Bub1 is not recruited to kinetochores, can be overcome by an excess of non-kinetochore bound Bub1 over Bub3. Together these results suggest that the toggle switch for the spindle checkpoint at kinetochores is not only dependent on the availability of phosphorylatable MELT motifs but also on the relative abundance of Bub1 and Bub3.

Bub3 inhibits Bub1-dependent SAC signalling when not bound to Spc7 (KNL1)

This prompted us to examine whether Bub3 acts as an inhibitor of Bub1 when not bound to kinetochores. Importantly, crystallographic data has revealed that the phosphorylated threonines in MELT motifs from the budding yeast KNL1 homologue, Spc105, form ionic bonds with the Bub3 β-propeller toroid and that mutation of Arg^{217} and Arg^{239} in Bub3 abolishes localisation of Bub3 and Bub1 to kinetochores and prevents budding yeast cells from mounting a spindle checkpoint response [7]. However, since Bub3 is also a component of the MCC in budding yeast, it is unclear whether checkpoint failure in this mutant is due to an inability of Bub3 to interact with Spc105, or because these mutations disrupt the structural integrity of the MCC complex, or both. Importantly, Bub3 is not essential for checkpoint activation and Bub3 is not a component of MCC in fission yeast [8]. For this reason we created a *bub3-R201A,K221A* mutant at the endogenous locus which, based on crystallography and homology, should be defective in binding phospho-MELT repeats of Spc7, but which would not influence MCC stability (Figure S2A; hereafter referred to as *bub3-RA,KA* mutant). In *bub3-RA,KA* cells, Bub1 remains in the nucleus but fails to accumulate at the kinetochore (Figure 2A), even though interaction of Bub1 with the Bub3-RA,KA mutant protein remains intact (Figure 2B). Consistently, the Bub3-RA,KA-GFP protein fails to localise to the kinetochore (Figure 2A). This is probably due to the inability of Bub3-Bub1 to interact with phosphorylated Spc7 MELT repeats since GST-Spc7-T9E proteins is unable to precipitate the Bub3-Bub1 complex from extracts of *bub3-RA,KA* cells (Figure 2C). Indeed no GFP foci were observed in interphase or mitotic *bub1-GFP bub3-RA,KA spc7-9TE* or *bub3-RA,KA-GFP spc7-9TE*

cells, indicating that interaction of the Bub3-Bub1 complex with phosphorylated Spc7 is disrupted in the *bub3-RA,KA* mutant (Figure 2A).

To our surprise expression of *bub3-RA,KA* from its endogenous locus displayed little defect in checkpoint signalling (Figure 2D). We noted, however, that the steady state level of the Bub3-RA,KA-GFP protein was approximately 40% lower than the corresponding Bub3-GFP wild type protein, as judged by western analysis (Figure 2E). To examine whether this accounted for the lack of effect of the *bub3-RA,KA* allele on checkpoint signalling, we integrated a second copy of the mutant *bub3-RA,KA* gene at the *lys1* locus. By itself (i.e. in a *Δbub3* background) the *lys1::bub3-RA,KA* allele also had only a minor effect on checkpoint signalling (Figure S2B). However, when both copies were expressed in the same cell (2x*bub3-RA,KA*), the total amount of the Bub3-RA,KA-GFP protein was 10% greater than that seen in wild type cells (Figure 2E) and the defect in checkpoint signalling was comparable to that observed in *spc7-9TA* cells (Figures 2D & 1C). Importantly, the checkpoint signalling defect in the 2x*bub3-RA,KA* mutant was suppressed in *bub1(ΔGLEBS)* cells, which lack the GLEBS domain in Bub1 that is required for Bub3 binding [9], or when a second copy of Bub1 (2Xbub1) was introduced indicating that, when not bound to phosphorylated MELT motifs, Bub3 exerts its dose-dependent inhibitory effect on checkpoint signalling through interaction with Bub1 (Figure 2D). The fact that checkpoint signalling is not completely abrogated in *spc7-12TA* or bub3-*RA,KA* mutants suggests that a fraction of Bub1 can escape the inhibitory effect of Bub3.

Mph1 (Mps1) kinase and Dis2 (PP1) phosphatase antagonistically regulate the interaction of Mad1-Mad2 with Bub1

We reasoned that kinetochore association of Bub3-Bub1 may relieve the inhibitory effect of Bub3 by altering interaction of Bub1 with other components of the spindle checkpoint. To test this, extracts were prepared from *nda3-KM311 bub1-6HA* cells expressing *mad1-GFP*, *mad2-GFP* or *mad3-GFP* and tested for co-immunoprecipitation. We find that Mad1, Mad2 and Mad3 all interact with Bub1 in checkpoint arrested cells, although the interaction between Mad1 and Bub1 is weak, possibly because the *mad1-GFP* allele is not fully functional (Figure 3A & S3A). Notably, interaction of Mad2 with Bub1 is observed in checkpoint arrested, but not log phase, cells whereas formation of Mad1-Mad2 and Mad3-Bub1 complexes are observed in both conditions, although this is

increased in checkpoint arrested cells (Figure 3B). In budding yeast, Mps1-mediated phosphorylation of Bub1 recruits Mad1-Mad2 complex to kinetochores and this is required for checkpoint signalling [5]. This prompted us to assess the phosphorylation requirements for interaction of Bub1 with Mad1, Mad2 and Mad3 in fission yeast. We find that in the absence of Dis2, the major form of type-1-phosphatase (PP1), interaction of both Mad1 and Mad2 with Bub1 is enhanced whereas, to our surprise, interaction of Mad3 with Bub1 was diminished (Figures 3C & S3B). Since cells lacking Mph1 kinase are checkpoint defective, we arrested *cdc25-22* allele cells in late G2 before releasing them synchronously into mitosis in the presence of CBZ, an inhibitor of microtubule polymerisation. Addition of CBZ completely blocked the onset of anaphase in control cells, but not in *Δmad3* cells, and only delayed anaphase onset in *spc7-12TA* cells by 5 minutes (Figure S3C). Importantly, we find that, as in budding yeast, interaction of Mad2 with Bub1 in CBZ treated prometaphase cells is dependent on Mph1 (Mps1) kinase (Figures 3D & S3D). We and others previously showed that localisation of Mad1 and Mad2 to kinetochores is dependent on a conserved RLK motif of Mad1 and a conserved central motif of Bub1 (cm1) [10-12]. The motif cm1 contains three conserved residues, Ser381, Thr383 and Thr386, which are phosphorylated in checkpoint arrested fission yeast cells (Hervas-Aguilar and Millar, unpublished data). Mutation of these residues (Bub1(SATATA)) abolishes recruitment of Mad1 and Mad2 to kinetochores and disables checkpoint signalling [10]. We find that association of both Mad1 and Mad2 to Bub1 also depends on these residues (Figure 3E & S3E) but interaction of Mad3 to Bub1 does not (Figure S3E). Together this indicates that Mph1 (Mps1) kinase and Dis2 (PP1) phosphatase antagonistically regulate the interaction of Mad1 and Mad2 with Bub1 in fission yeast, likely through phosphorylation of the conserved central motif of Bub1.

Bub3 licenses phospho-dependent interaction of Bub1 with the Mad1-Mad2 complex

We next sought to understand how kinetochore association of Bub3-Bub1 protein influences checkpoint signalling. In fission yeast, Bub3 is not required for spindle checkpoint arrest as Bub3 is not a component of MCC but, instead, is necessary for efficient checkpoint activation and silencing [8, 13, 14]. Indeed, Bub1 interacts with both Mad2 and Mad3 in checkpoint arrested cells lacking Bub3 (Figure 4A). This suggests that Bub3 is not strictly required for interaction of Mad1-Mad2 complex with Bub1. Notably, however, we find that interaction of Mad2 with Bub1 is drastically

reduced in *spc7-12TA* cells compared to wild type cells, while the interaction of Mad3 with Bub1 increased (Figures 4B & S4A). Importantly, the interaction of Mad1 and Mad2 with Bub1 in *spc7-12TA* is restored by deletion of Bub3, indicating that Bub3 acts as a negative regulator of Bub1:Mad2 interaction when it is not bound at kinetochores (Figure 4C & S4B). Conversely, deletion of Bub3 decreases interaction of Mad3 with Bub1 in *spc7-12TA* cells (Figure S4C). This antagonistic relationship suggests Mad3 may participate in Bub3-dependent regulation of Mad1-Mad2 binding to Bub1. Identification of Mad3 mutants that specifically fail to associate to Bub1, but retain the ability to form MCC, would help clarify this issue.

Taken together, our data indicate that the Spc7 (KNL1) MELT array acts as a multisite phospho-dependent toggle switch for the spindle checkpoint at kinetochores, which relies on conversion of Bub3 from an inhibitor to a facilitator of spindle checkpoint signalling by controlling the interaction of Mad1-Mad2 with Bub1. Once occupancy of Spc7 (KNL1) by Bub3-Bub1 drops below a critical threshold, the rate of MCC generation drops below the rate of MCC turnover, permitting APC/C activation and anaphase onset. This would explain why kinetochore binding of Bub3-Bub1 reduces as cells enter metaphase, but does not completely disappear until late anaphase. We postulate that, just like Mad2, Bub3-Bub1 undergoes a conformational change, that is dependent on its interaction with phosphorylated MELT motifs of Spc7 (KNL1), which permits the interaction of Mad1-Mad2 with Bub1 (Figure 4D). Reconstitution and structural studies will be needed to test this hypothesis. Importantly, in human cells, the spindle checkpoint behaves like a rheostat, rather than as a toggle switch, in response to increasing levels of microtubule-kinetochore detachment [15, 16]. This is seemingly at odds with the finding that only a small number of MELT motifs in KNL1 are needed to mount a checkpoint response [17-19]. However, these latter experiments were performed in the presence of reversine, an inhibitor of Mps1 kinase. More recent analysis indicates that human cells possess two distinct means to recruit the Mad1-Mad2 complex to kinetochores; the KNL1-Bub3-Bub1 (KBB) pathway and a second, KNL1-independent, mechanism mediated by the RZZ-Spindly complex, which absent in yeast [20]. One possibility, that merits further analysis, is that the RZZ-spindly complex obscures the switch like behaviour of the KBB pathway, which is only revealed in the presence of reversine. We contend that modulation of Bub3 levels by BuGZ [21, 22] or phosphorylation of Bub3 by PKM2 kinase [23] or simply alteration of kinetochore number (and therefore number of MELT motifs) influences either the threshold or

amplitude of the KBB toggle switch and, in doing so, contributes to chromosome instability in aneuploid cancer cells.

Experimental Procedures

Detailed in Supplemental Information.

Author Contributions

Project was conceived by J.B.M. All experiments were carried out by M.M.S. with the exception of single cell analysis of Bub1 and Bub3 binding to the kinetochore (J.C.M.) and single cell checkpoint response (K.S.). A.H-A. and T.C.L. aided with molecular biology and strain construction. The manuscript was written by J.B.M. with help from M.M.S., K.S. and J.C.M.

Acknowledgements

We thank Andrew McAinsh for critical reading of the manuscript. This work was supported by a program grant (MR/K001000/1) from the Medical Research Council UK (J.B.M.), a Global Research Fellowship from the Warwick Institute of Advanced Study (J.C.M.) and funds from Virginia Tech (K.S.).

References

1. Musacchio, A. (2015). The Molecular Biology of Spindle Assembly Checkpoint Signaling Dynamics. Curr Biol *25*, R1002-1018.
2. London, N., Ceto, S., Ranish, J.A., and Biggins, S. (2012). Phosphoregulation of Spc105 by Mps1 and PP1 regulates Bub1 localization to kinetochores. Curr Biol *22*, 900-906.
3. Shepperd, L.A., Meadows, J.C., Sochaj, A.M., Lancaster, T.C., Zou, J., Buttrick, G.J., Rappsilber, J., Hardwick, K.G., and Millar, J.B. (2012). Phosphodependent recruitment of Bub1 and Bub3 to Spc7/KNL1 by Mph1 kinase maintains the spindle checkpoint. Curr Biol *22*, 891-899.

4. Yamagishi, Y., Yang, C.H., Tanno, Y., and Watanabe, Y. (2012). MPS1/Mph1 phosphorylates the kinetochore protein KNL1/Spc7 to recruit SAC components. Nat Cell Biol *14*, 746-752.

5. London, N., and Biggins, S. (2014). Mad1 kinetochore recruitment by Mps1-mediated phosphorylation of Bub1 signals the spindle checkpoint. Genes Dev *28*, 140-152.

6. Heinrich, S., Geissen, E.M., Kamenz, J., Trautmann, S., Widmer, C., Drewe, P., Knop, M., Radde, N., Hasenauer, J., and Hauf, S. (2013). Determinants of robustness in spindle assembly checkpoint signalling. Nat Cell Biol *15*, 1328-1339.

7. Primorac, I., Weir, J.R., Chiroli, E., Gross, F., Hoffmann, I., van Gerwen, S., Ciliberto, A., and Musacchio, A. (2013). Bub3 reads phosphorylated MELT repeats to promote spindle assembly checkpoint signaling. Elife *2*, e01030.

8. Vanoosthuyse, V., Meadows, J.C., van der Sar, S.J., Millar, J.B., and Hardwick, K.G. (2009). Bub3p facilitates spindle checkpoint silencing in fission yeast. Mol Biol Cell *20*, 5096-5105.

9. Wang, X., Babu, J.R., Harden, J.M., Jablonski, S.A., Gazi, M.H., Lingle, W.L., de Groen, P.C., Yen, T.J., and van Deursen, J.M. (2001). The mitotic checkpoint protein hBUB3 and the mRNA export factor hRAE1 interact with GLE2p-binding sequence (GLEBS)-containing proteins. J Biol Chem *276*, 26559-26567.

10. Heinrich, S., Sewart, K., Windecker, H., Langegger, M., Schmidt, N., Hustedt, N., and Hauf, S. (2014). Mad1 contribution to spindle assembly checkpoint signalling goes beyond presenting Mad2 at kinetochores. EMBO Rep *15*, 291-298.

11. Klebig, C., Korinth, D., and Meraldi, P. (2009). Bub1 regulates chromosome segregation in a kinetochore-independent manner. J Cell Biol *185*, 841-858.

12. Kim, S., Sun, H., Tomchick, D.R., Yu, H., and Luo, X. (2012). Structure of human Mad1 C-terminal domain reveals its involvement in kinetochore targeting. Proc Natl Acad Sci U S A *109*, 6549-6554.

13. Tange, Y., and Niwa, O. (2008). Schizosaccharomyces pombe Bub3 is dispensable for mitotic arrest following perturbed spindle formation. Genetics *179*, 785-792.

14. Windecker, H., Langegger, M., Heinrich, S., and Hauf, S. (2009). Bub1 and Bub3 promote the conversion from monopolar to bipolar chromosome attachment independently of shugoshin. EMBO Rep *10*, 1022-1028.

15. Collin, P., Nashchekina, O., Walker, R., and Pines, J. (2013). The spindle assembly checkpoint works like a rheostat rather than a toggle switch. Nat Cell Biol *15*, 1378-1385.

16. Dick, A.E., and Gerlich, D.W. (2013). Kinetic framework of spindle assembly checkpoint signalling. Nat Cell Biol *15*, 1370-1377.

17. Vleugel, M., Tromer, E., Omerzu, M., Groenewold, V., Nijenhuis, W., Snel, B., and Kops, G.J. (2013). Arrayed BUB recruitment modules in the kinetochore scaffold KNL1 promote accurate chromosome segregation. J Cell Biol *203*, 943-955.

18. Zhang, G., Lischetti, T., and Nilsson, J. (2014). A minimal number of MELT repeats supports all the functions of KNL1 in chromosome segregation. J Cell Sci *127*, 871-884.

19. Krenn, V., Overlack, K., Primorac, I., van Gerwen, S., and Musacchio, A. (2014). KI motifs of human Knl1 enhance assembly of comprehensive spindle checkpoint complexes around MELT repeats. Curr Biol *24*, 29-39.

20. Silio, V., McAinsh, A.D., and Millar, J.B. (2015). KNL1-Bubs and RZZ Provide Two Separable Pathways for Checkpoint Activation at Human Kinetochores. Dev Cell *35*, 600-613.

21. Jiang, H., He, X., Wang, S., Jia, J., Wan, Y., Wang, Y., Zeng, R., Yates, J., 3rd, Zhu, X., and Zheng, Y. (2014). A microtubule-associated zinc finger protein, BuGZ, regulates mitotic chromosome alignment by ensuring Bub3 stability and kinetochore targeting. Dev Cell *28*, 268-281.

22. Toledo, C.M., Herman, J.A., Olsen, J.B., Ding, Y., Corrin, P., Girard, E.J., Olson, J.M., Emili, A., DeLuca, J.G., and Paddison, P.J. (2014). BuGZ is required for Bub3 stability, Bub1 kinetochore function, and chromosome alignment. Dev Cell *28*, 282-294.

23. Jiang, Y., Li, X., Yang, W., Hawke, D.H., Zheng, Y., Xia, Y., Aldape, K., Wei, C., Guo, F., Chen, Y., et al. (2014). PKM2 regulates chromosome segregation and mitosis progression of tumor cells. Mol Cell *53*, 75-87.

Figure Legends

Figure 1. Levels of Bub1-Bub3 at kinetochores threshold the activity of the spindle assembly checkpoint

(A) Bub1 bound to kinetochores decreases as MELT motifs are abolished. Levels of Bub1-GFP, normalised against inner kinetochore Fta3-RFP, were calculated in individual *spc7-mutant* cells arrested in mitosis by overexpression of Mad2. Representative images are shown in the right panel. Bar, 1 μm. **(B)** Switch-like checkpoint response of the Spc7 MELT array. The duration of mitosis prior to anaphase was determined by live cell imaging of Plo1-GFP in individual *nda3-KM311 spc7-mutant* cells at the restrictive temperature. **(C)** Anaphase onset was determined by measuring the appearance of Nsk1-GFP at the times indicated in *nda3-KM11 nsk1-gfp spc7-mutant* cells. **(D)** An extra copy of Bub1 rescues the checkpoint defect in *spc7-12TA* cells. Log phase cultures of the illustrated strains were treated as in (C). Dashed line indicates the same control culture data as in (C). See also Figure S1.

Figure 2. Bub3 inhibits the spindle checkpoint when it is not bound at kinetochores

(A) Bub1 and Bub3 do not bind the kinetochore in *bub3-R201A,K221A* mutant cells. Log phase cultures of wild type (left panels) or *spc7-T9E* cells (right panels) expressing *sid4-TdTomato* were fixed and the percentage of cells with a < 2 μm mitotic spindle (left panels: Bar, 1 μm) or the percentage of all *spc7-9TE* cells (right panels: Bar, 5 μm) that were positive for GFP foci determined. Filled arrowheads indicate mitotic cells with GFP foci and open arrowheads those without. **(B)** Bub1 interacts with Bub3-RA,KA *in vivo*. Log phase NP-40 extracts from the indicated strains were immunoprecipitated with rabbit anti-GFP (I) or normal rabbit serum (PI). Complexes were analysed by immunoblot using anti-HA or sheep anti-GFP antibodies. **(C)** Bub3-RA,KA does not interact with Spc7-9TE *in vitro*. Fusion proteins, purified by Sepharose beads (left panel), were incubated with the indicated extracts and analysed by immunoblot using anti-HA or anti-sheep GFP antibodies (right panel). (Mw) Molecular weight marker. **(D)** Maintenance of the spindle checkpoint is defective in *2xbub3(RA,KA)* cells. The indicated *nda3-KM11* strains were fixed at the times shown and the percentage of anaphase cells (Nsk1-GFP positive) determined. **(E)** Bub3-RA,KA is less stable than Bub3. Extracts from the indicated cells were analysed by immunoblotting using

sheep anti-GFP and anti-Tat1 (tubulin) antibodies. Quantification of normalised GFP levels is shown (Bub3 RA,KA-GFP ±0.185; 2XBub3 RA,KA-GFP ±0.23 (±SD)). See also Figure S2.

Figure 3. The mitotic interaction between Mad2 and Bub1 is antagonistically regulated by Mph1 kinase and Dis2 (PP1) phosphatase

(A) Bub1 interacts with both Mad2 and Mad3 *in vivo*. Following incubation at 18 ºC for 6 hours, extracts were prepared from the illustrated strains and then immunoprecipitated with rabbit anti-GFP (I) or normal rabbit serum *(*PI) and complexes analysed by immunoblot using anti-HA, rabbit anti-Mad1 and sheep anti-GFP antibodies. **(B)** Bub1 and Mad2 interact specifically in mitosis. The indicated cells were incubated at either 30 ºC or 18 ºC for 6 hours and then immunoprecipited as in (A). **(C)** Bub1 interactions with Mad2 and Mad3 are differentially regulated by PP1. The indicated strains were treated and analysed as in (A). Quantification of normalised Bub1-6HA levels is shown (± SD). **(D)** Mph1 kinase is required for Bub1 to interact with Mad2. The strains shown were shifted to 35.5 ºC for 4 hours and released at 25 ºC. After 10 min, CBZ was added at 200 µg/ml and cells collected 15 min later. Extracts were immunoprecipitated and analysed as in (A). **(E)** Bub1-conserved motif 1 (cm1) is required for its interaction with Mad2. The indicated strains were treated and analysed as in (D). (Mw) Molecular weight marker. Migration of molecular markers (in kilodaltons) is shown to the left of each blot. 5% input of NP-40 yeast extracts (E). Asterisks indicate unspecific binding. See also Figure S3.

Figure 4. Bub3 regulates the interaction between Mad2 and Bub1 differentially at the kinetochore or in the nucleoplasm

(A) Bub1 interacts with Mad2 and Mad3 in the absence of Bub3. The indicated strains were incubated for 4 hours at 18 ºC. Extracts were prepared and immunoprecipitated with rabbit anti-GFP (I) or normal rabbit serum (PI) and analysed by immunoblot using anti-HA, rabbit anti-Mad1 and sheep anti-GFP antibodies. **(B)** Altering kinetochore binding of Bub1 affects its interaction with Mad2 and Mad3 differentially. Indicated strains were treated and analysed as in (A). **(C)** Bub3 inhibits the interaction between Bub1 and Mad2 in the nucleoplasm. Indicated strains were treated and analysed as in (A). **(D)** Model to illustrate how spindle checkpoint regulation is altered by kinetochore-bound or non-kinetochore-bound interactions. Bub3 at the kinetochore (left panel)

allows formation of a Bub1-Mad1-Mad2 complex that can efficiently catalyse C-Mad2 formation and arrest anaphase. When kinetochore recruitment is disrupted (middle panel) by MELT motif or Bub3 mutation, Bub1 interaction with Mad1-Mad2 is abolished resulting in the failure to generate an inhibitory signal and anaphase onset. Checkpoint functionality can be restored, however, by either deleting Bub3, allowing interaction between Bub1 and Mad1-Mad2 in the nucleoplasm, or by increasing the amount of Bub1 to effectively titrate out Bub3 (right panels). (Mw) Molecular weight marker. Migration of molecular markers (in kilodaltons) is shown to the left of each blot. 5% input of NP-40 yeast extracts (E). Quantification of normalised Bub1-6HA levels is shown (±SD). Asterisks indicate unspecific binding. See also Figure S4.

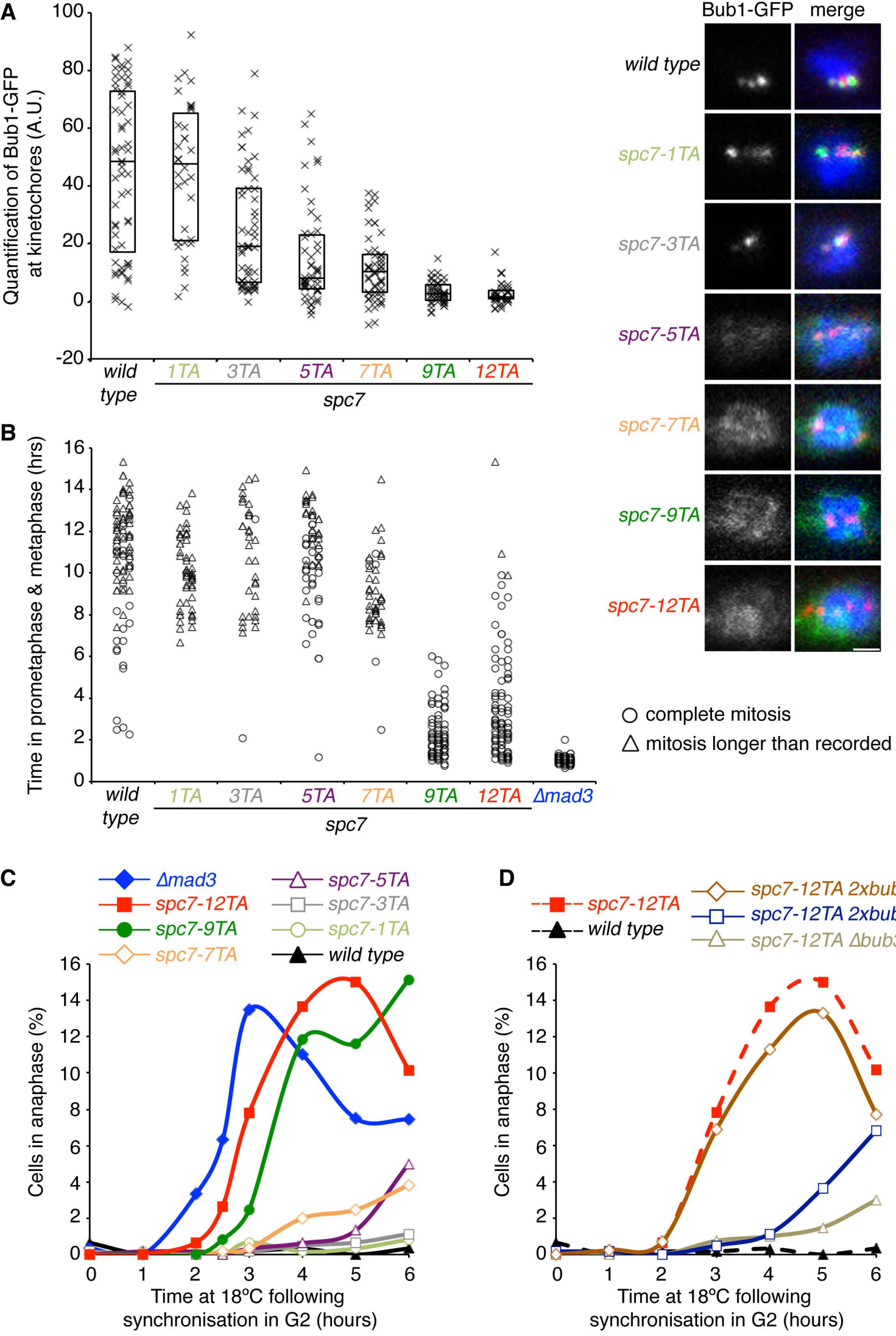
A
Quantification of Bub1-GFP at kinetochores (A.U.)
100
80
60
40
20
0
-20
wild type
1TA
3TA
5TA
7TA
9TA
12TA
spc7
Bub1-GFP
merge
wild type
spc7-1TA
spc7-3TA
spc7-5TA
spc7-7TA
spc7-9TA
spc7-12TA
B
Time in prometaphase & metaphase (hrs)
16
14
12
10
8
6
4
2
0
wild type
1TA
3TA
5TA
7TA
9TA
12TA
Δmad3
spc7
complete mitosis
mitosis longer than recorded
C
Δmad3
spc7-12TA
spc7-9TA
spc7-7TA
spc7-5TA
spc7-3TA
spc7-1TA
wild type
Cells in anaphase (%)
16
14
12
10
8
6
4
2
0
0
1
2
3
4
5
6
Time at 18ºC following synchronisation in G2 (hours)
D
spc7-12TA
wild type
spc7-12TA 2xbub3
spc7-12TA 2xbub1
spc7-12TA Δbub3
Cells in anaphase (%)
16
14
12
10
8
6
4
2
0
0
1
2
3
4
5
6
Time at 18ºC following synchronisation in G2 (hours)

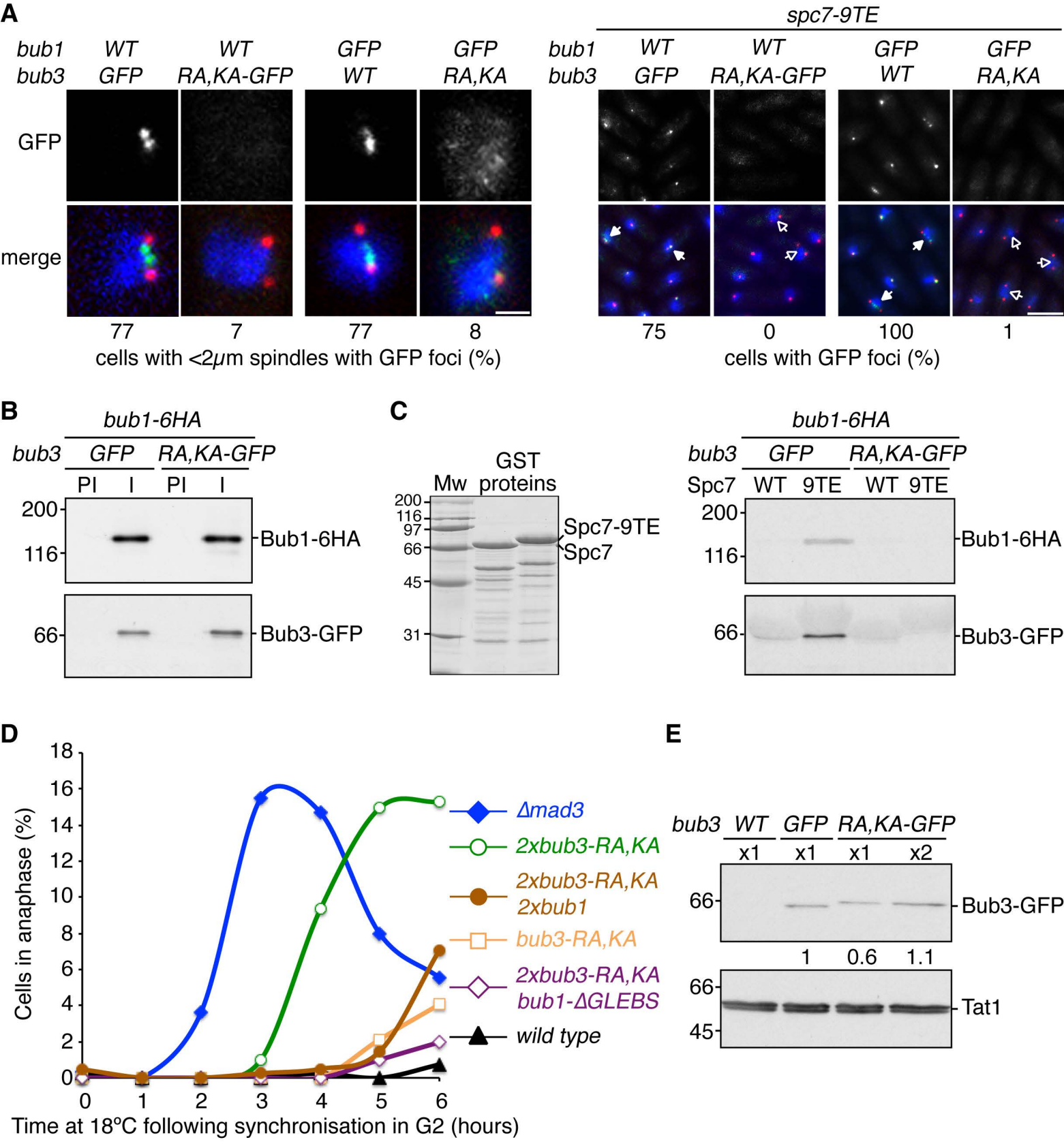
A
spc7-9TE
bub1 bub3
WT GFP
WT RA,KA-GFP
GFP WT
GFP RA,KA
GFP
merge
77
7
77
8
cells with <2μm spindles with GFP foci (%)
75
0
100
1
cells with GFP foci (%)
B
bub1-6HA
bub3
GFP
RA,KA-GFP
PI
I
200
116
66
Bub1-6HA
Bub3-GFP
C
GST proteins
Mw
200
116
97
66
45
31
Spc7-9TE
Spc7
Spc7
WT
9TE
D
Cells in anaphase (%)
Time at 18°C following synchronisation in G2 (hours)
Δmad3
2xbub3-RA,KA
2xbub3-RA,KA 2xbub1
bub3-RA,KA
2xbub3-RA,KA bub1-ΔGLEBS
wild type
E
x1
x2
1
0.6
1.1
Tat1

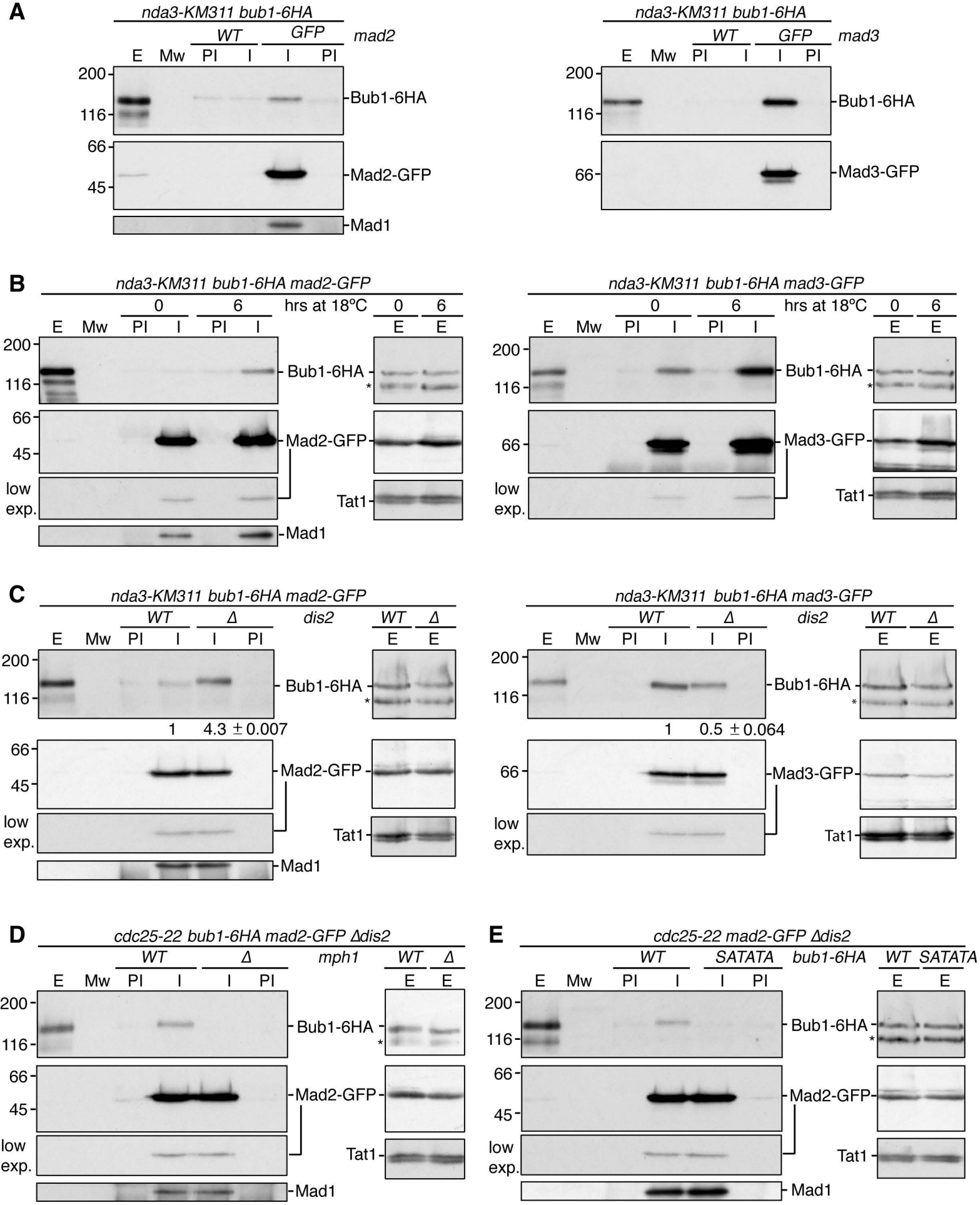
A
nda3-KM311 bub1-6HA
WT
GFP
mad2
E Mw PI I I PI
200
116
66
45
Bub1-6HA
Mad2-GFP
Mad1
nda3-KM311 bub1-6HA
WT
GFP
mad3
E Mw PI I I PI
200
116
66
Bub1-6HA
Mad3-GFP
B
nda3-KM311 bub1-6HA mad2-GFP
0
6
hrs at 18ºC
0
6
E Mw PI I PI I
E E
200
116
66
45
low exp.
Bub1-6HA
Mad2-GFP
Mad1
Tat1
nda3-KM311 bub1-6HA mad3-GFP
0
6
hrs at 18ºC
0
6
E Mw PI I PI I
E E
200
116
66
low exp.
Bub1-6HA
Mad3-GFP
Tat1
C
nda3-KM311 bub1-6HA mad2-GFP
WT
Δ
dis2
WT
Δ
E Mw PI I I PI
E E
200
116
1 4.3 ± 0.007
66
45
low exp.
Bub1-6HA
Mad2-GFP
Mad1
Tat1
nda3-KM311 bub1-6HA mad3-GFP
WT
Δ
dis2
WT
Δ
E Mw PI I I PI
E E
200
116
1 0.5 ± 0.064
66
low exp.
Bub1-6HA
Mad3-GFP
Tat1
D
cdc25-22 bub1-6HA mad2-GFP Δdis2
WT
Δ
mph1
WT
Δ
E Mw PI I I PI
E E
200
116
66
45
low exp.
Bub1-6HA
Mad2-GFP
Mad1
Tat1
E
cdc25-22 mad2-GFP Δdis2
WT
SATATA
bub1-6HA
WT
SATATA
E Mw PI I I PI
E E
200
116
66
45
low exp.
Bub1-6HA
Mad2-GFP
Mad1
Tat1

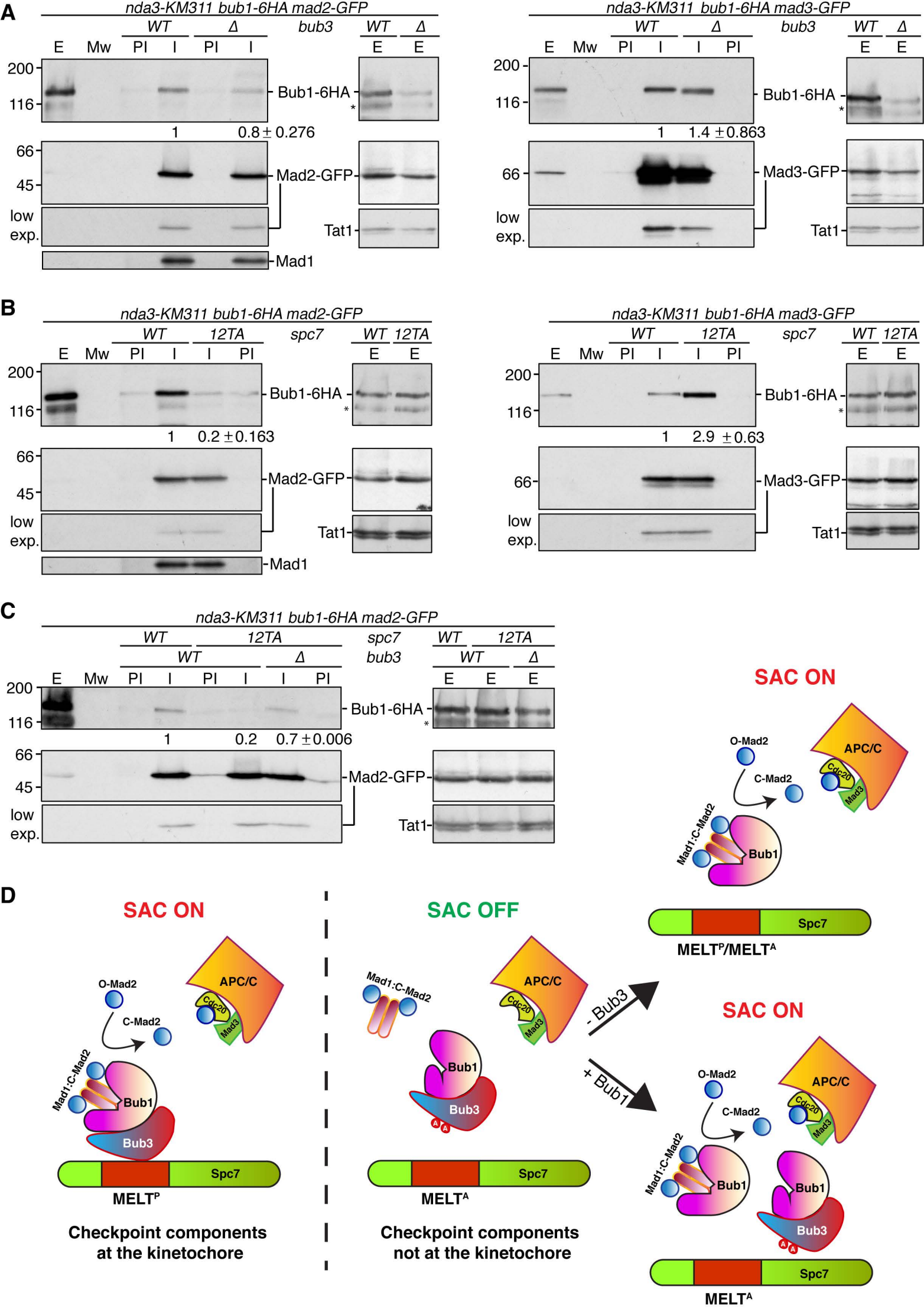
A
nda3-KM311 bub1-6HA mad2-GFP
WT
Δ
bub3
E
Mw
Pl
I
200
116
66
45
low exp.
Bub1-6HA
1
0.8 ± 0.276
Mad2-GFP
Tat1
Mad1
nda3-KM311 bub1-6HA mad3-GFP
1
1.4 ± 0.863
Mad3-GFP
B
nda3-KM311 bub1-6HA mad2-GFP
12TA
spc7
0.2 ± 0.163
nda3-KM311 bub1-6HA mad3-GFP
2.9 ± 0.63
C
nda3-KM311 bub1-6HA mad2-GFP
0.2
0.7 ± 0.006
SAC ON
O-Mad2
C-Mad2
APC/C
Cdc20
Mad3
Mad1:C-Mad2
Bub1
D
SAC ON
Bub3
Spc7
MELTP
Checkpoint components at the kinetochore
SAC OFF
MELTP/MELTA
- Bub3
+ Bub1
MELTA
Checkpoint components not at the kinetochore

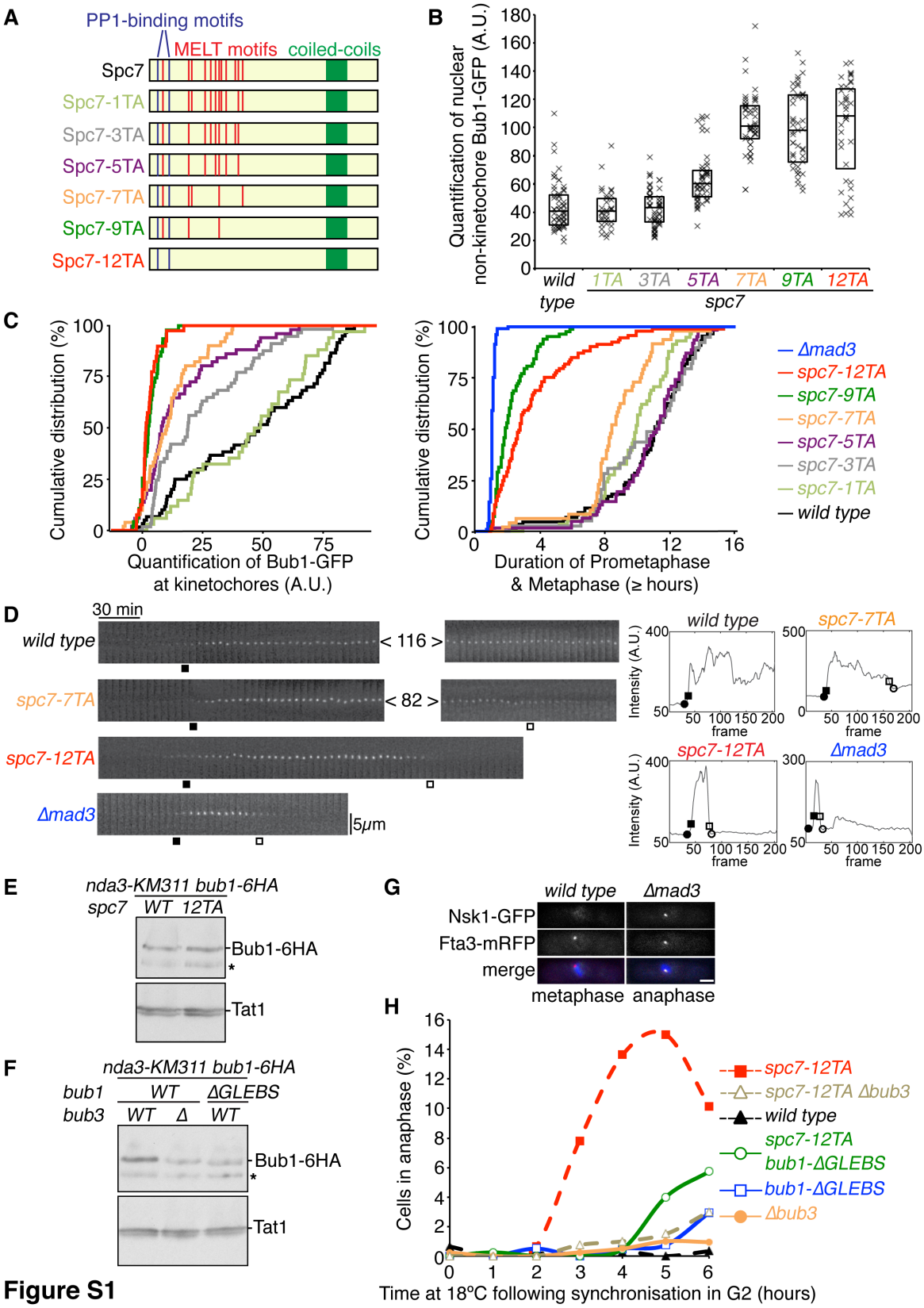
A
PP1-binding motifs
MELT motifs
coiled-coils
Spc7
Spc7-1TA
Spc7-3TA
Spc7-5TA
Spc7-7TA
Spc7-9TA
Spc7-12TA
B
Quantification of nuclear non-kinetochore Bub1-GFP (A.U.)
wild type
1TA
3TA
5TA
7TA
9TA
12TA
spc7
C
Cumulative distribution (%)
Quantification of Bub1-GFP at kinetochores (A.U.)
Duration of Prometaphase & Metaphase (≥ hours)
Δmad3
spc7-12TA
spc7-9TA
spc7-7TA
spc7-5TA
spc7-3TA
spc7-1TA
wild type
D
30 min
wild type
spc7-7TA
spc7-12TA
Δmad3
5μm
Intensity (A.U.)
frame
E
nda3-KM311 bub1-6HA
spc7 WT 12TA
Bub1-6HA
Tat1
F
nda3-KM311 bub1-6HA
bub1 WT ΔGLEBS
bub3 WT Δ WT
Bub1-6HA
Tat1
G
wild type
Δmad3
Nsk1-GFP
Fta3-mRFP
merge
metaphase
anaphase
H
Cells in anaphase (%)
Time at 18ºC following synchronisation in G2 (hours)
spc7-12TA
spc7-12TA Δbub3
wild type
spc7-12TA bub1-ΔGLEBS
bub1-ΔGLEBS
Δbub3

Figure S1

A

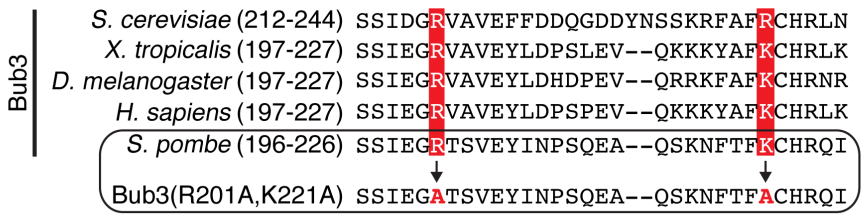
Bub3
S. cerevisiae (212-244) SSIDGRVAVEFFDDQGDDYNSSKRFAFRCHRLN
X. tropicalis (197-227) SSIEGRVAVEYLDPSLEV--QKKKYAFKCHRLK
D. melanogaster (197-227) SSIEGRVAVEYLDHDPEV--QRRKFAFKCHRNR
H. sapiens (197-227) SSIEGRVAVEYLDPSPEV--QKKKYAFKCHRLK
S. pombe (196-226) SSIEGRTSVEYINPSQEA--QSKNFTFKCHRQI
Bub3(R201A,K221A) SSIEGATSVEYINPSQEA--QSKNFTFACHRQI

B

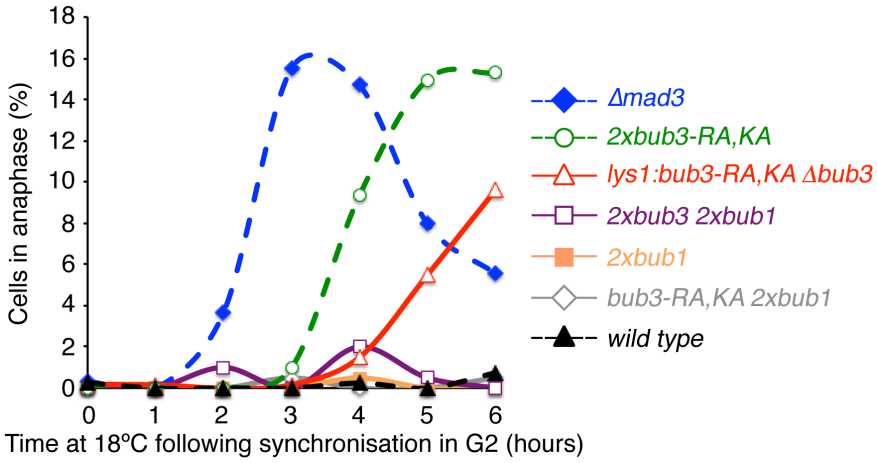
Cells in anaphase (%)
18
16
14
12
10
8
6
4
2
0
0 1 2 3 4 5 6
Time at 18ºC following synchronisation in G2 (hours)
Δmad3
2xbub3-RA,KA
lys1:bub3-RA,KA Δbub3
2xbub3 2xbub1
2xbub1
bub3-RA,KA 2xbub1
wild type

Figure S2

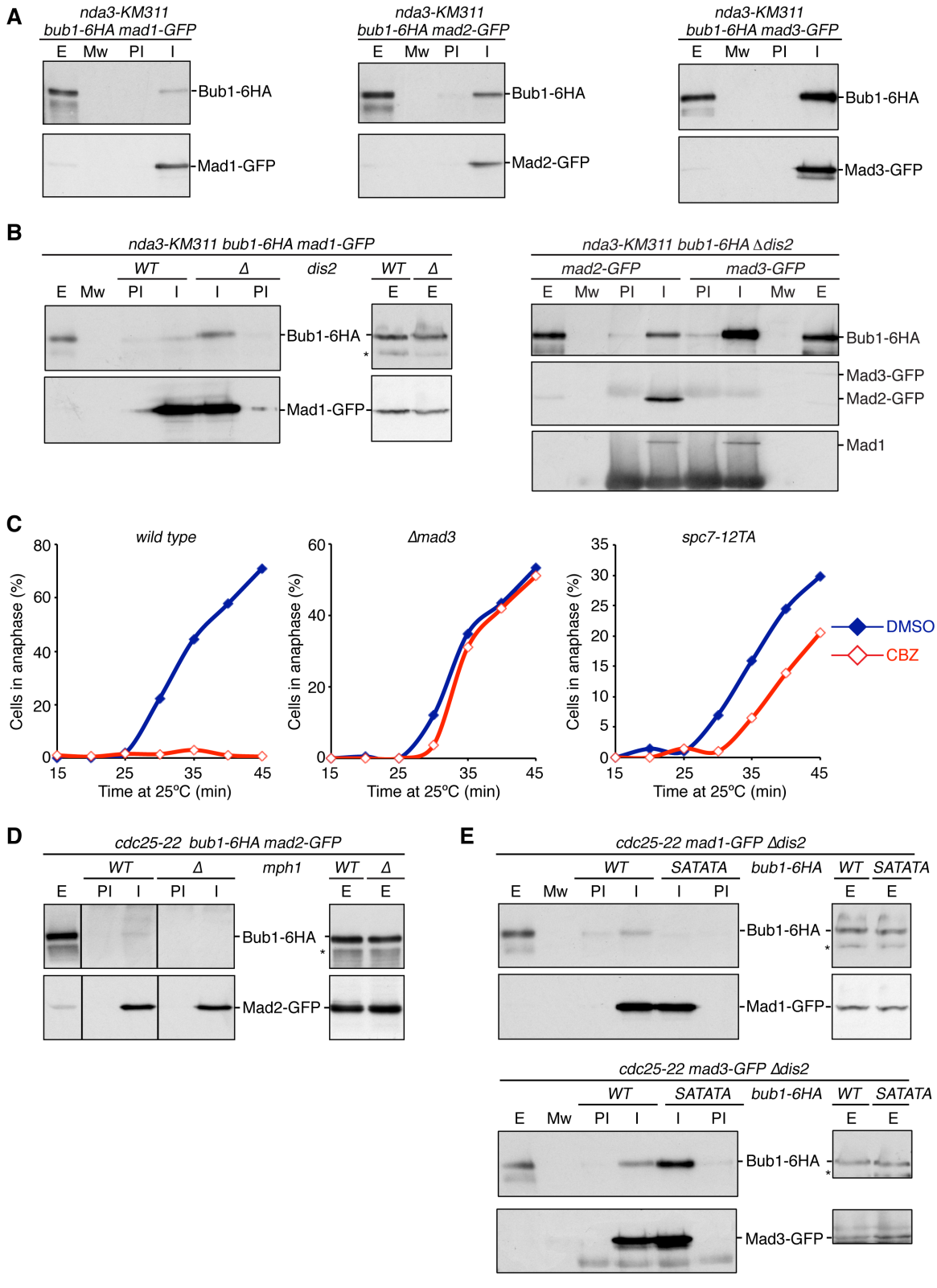
A
nda3-KM311 bub1-6HA mad1-GFP
E Mw PI I
Bub1-6HA
Mad1-GFP
nda3-KM311 bub1-6HA mad2-GFP
E Mw PI I
Bub1-6HA
Mad2-GFP
nda3-KM311 bub1-6HA mad3-GFP
E Mw PI I
Bub1-6HA
Mad3-GFP
B
nda3-KM311 bub1-6HA mad1-GFP
WT Δ dis2 WT Δ
E Mw PI I I PI E E
Bub1-6HA
Mad1-GFP
nda3-KM311 bub1-6HA Δdis2
mad2-GFP mad3-GFP
E Mw PI I PI I Mw E
Bub1-6HA
Mad3-GFP
Mad2-GFP
Mad1
C
wild type
Δmad3
spc7-12TA
Cells in anaphase (%)
Time at 25°C (min)
DMSO
CBZ
D
cdc25-22 bub1-6HA mad2-GFP
WT Δ mph1 WT Δ
E PI I PI I E E
Bub1-6HA
Mad2-GFP
E
cdc25-22 mad1-GFP Δdis2
WT SATATA bub1-6HA WT SATATA
E Mw PI I I PI E E
Bub1-6HA
Mad1-GFP
cdc25-22 mad3-GFP Δdis2
WT SATATA bub1-6HA WT SATATA
E Mw PI I I PI E E
Bub1-6HA
Mad3-GFP

Figure S3

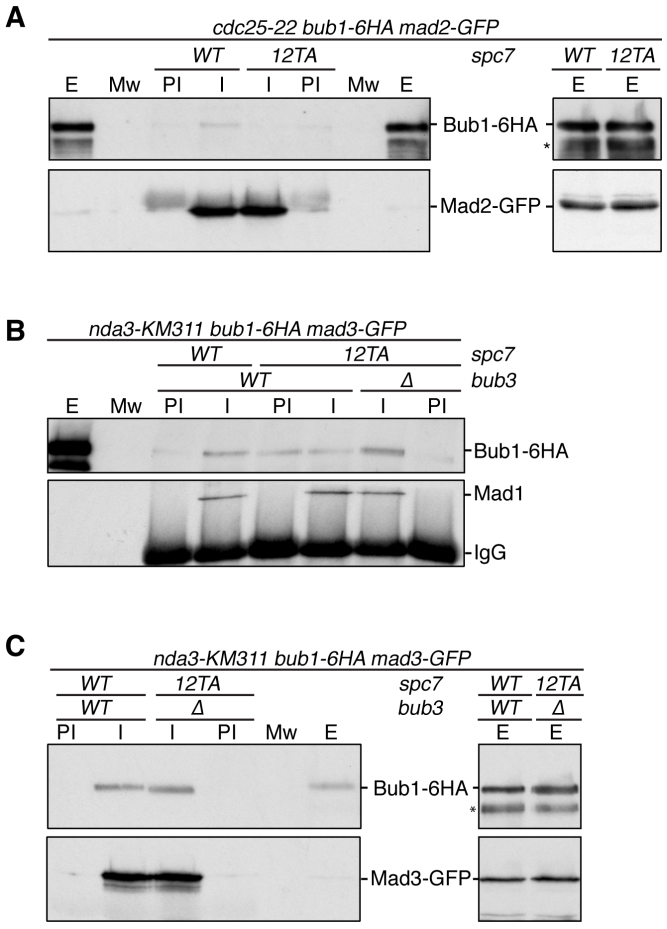
A
cdc25-22 bub1-6HA mad2-GFP
WT
12TA
spc7
WT
12TA
E
Mw
PI
I
I
PI
Mw
E
E
E
Bub1-6HA
*
Mad2-GFP
B
nda3-KM311 bub1-6HA mad3-GFP
WT
12TA
spc7
WT
Δ
bub3
E
Mw
PI
I
PI
I
I
PI
Bub1-6HA
Mad1
IgG
C
nda3-KM311 bub1-6HA mad3-GFP
WT
12TA
spc7
WT
12TA
WT
Δ
bub3
WT
Δ
PI
I
I
PI
Mw
E
E
E
Bub1-6HA
*
Mad3-GFP

Figure S4

Supplemental Figure Legends

Figure S1, related to Figure 1
(A) Diagram showing wild type Spc7 and the mutant alleles used in this study. Red lines indicate unmutated MELT motifs. **(B)** *bub1-GFP fta3-RFP pREP3x-mad2* cells expressing the *spc7* mutant alleles illustrated or wild type *spc7* were grown to mid-log phase in the presence of thiamine and then arrested in metaphase by growing in the absence of thiamine for 18 hours. Following fixation, the level of Bub1-GFP in the nucleus but not at kinetochores was calculated in individual cells. **(C)** Graphs to show the cumulative distributions of the data from Figures 1A (left panel) and 1B (right panel). (**D**) (Left panel) Kymographs of the spindle region of representative mitotic cells expressing the tubulin mutant *nda3-KM311* and *plo1-GFP* from Figure 1B. Cells were followed by live-cell microscopy at 16°C and Plo1-GFP appearance highlighted by closed squares and its disappearance by open squares. The *wild type* cell still showed a localized Plo1-GFP signal when recording was stopped. Frames removed for space constraints are represented as <n>. Time between frames: 5 minutes. (Right panel) Graphs show Plo1-GFP maximum intensity over time for the representative cells shown. Points indicated by circles and squares were determined by a custom MATLAB script. Closed circles mark the time-point before the first strong increase in Plo1-GFP signal and open circles the one after the last strong decrease. Time points where Plo1-GFP intensity increases above (closed squares) or decreases below (open squares) 1.3x the baseline and are used to determine the time spent in mitosis. **(E)** *nda3-KM311 bub1-6HA mad2-GFP* cells in the presence and absence of Spc7-12TA were grown to mid log phase before shifting to 18 ºC for 4 hours to arrest in mitosis and then harvested. NP-40 extracts were separated by SDS-PAGE and analysed by immunoblotting using anti-HA and anti-Tat1 antibodies. **(F)** Log phase cultures of *bub1-6HA*, *bub1-6HA Δbub3* and *bub1(ΔGLEBS)-6HA* cells expressing *nda3-KM311 mad2-GFP* were arrested in mitosis for 6 hours at 18 ºC and then harvested. NP-40 extracts were separated by SDS-PAGE and analysed by immunoblotting using anti-HA and anti-Tat1 antibodies. **(G)** Representative cells expressing the tubulin mutant *nda3-KM311* and the anaphase marker *nsk1-GFP* in the presence and absence of Mad3 from Figure 1C were grown to mid log phase before being synchronised in G2 by lactose gradient and incubated at 18 ºC for 3 hours. Bar, 2µm. **(H)** Log phase cultures of the illustrated strains expressing *nda3-KM311 nsk1-GFP* were synchronised in G2 by lactose gradient and incubated at 18 ºC for the times indicated. Cells were fixed and the percentage of anaphase cells (Nsk1-GFP positive) determined. Dashed lines indicate control data reproduced from Figure 1D. Asterisks indicate unspecific binding.

Figure S2, related to Figure 2
(A) Alignment of Bub3 from the indicated organisms. **(B)** Log phase cultures of the illustrated strains expressing *nda3-KM311 nsk1-GFP* were synchronised in G2 by lactose gradient and incubated at 18 ºC for the times indicated. Cells were fixed and the percentage of anaphase cells (Nsk1-GFP positive) determined. Dashed lines indicate control data reproduced from Figure 2D.

Figure S3, related to Figure 3
(A) Following incubation for 6 hours at 18 ºC to arrest in mitosis, NP-40 extracts were prepared from *mad1-GFP*, *mad2-GFP* and *mad3-GFP* strains expressing *nda3-KM311 bub1-6HA*. These were then immunoprecipitated with rabbit anti-GFP (I) or rabbit serum (PI) and complexes analysed by immunoblot using anti-HA and sheep anti-GFP. **(B)** Log phase cultures of *mad1-GFP, mad2-GFP* or *mad3-GFP* cells expressing *nda3-KM311 bub1-6HA* and either $dis2^+$ or Δ*dis2* were treated as in (A). Extracts of *mad2-GFP* or *mad3-GFP* cells expressing *nda3-KM311 bub1-6HA* and either $dis2^+$ or Δ*dis2* were inmunoprecipitated with rabbit anti-Mad1(I) or rabbit serum (PI) and complexes analysed by immonoblot using anti-HA, sheep anti-GFP and rabbit anti-Mad1 antibody. **(C)** *sid4-tdTomato cdc25-22* cells in the presence or absence of Mad3 and Spc7-12TA were grown to mid log phase before shifting to 35.5 ºC for 4 hours to arrest at the G2/M boundary. This was followed by release at 25 ºC. After 10 min, either CBZ at 200 µg/ml or an equal volume of DMSO was added and cells fixed at the times indicated. The percentage of anaphase cells (Nsk1-GFP positive) was determined. **(D)** Mid log phase *bub1-6HA mad2-GFP cdc25-22* strains expressing either *mph1* or *Δmph1* were shifted to 35.5 ºC for 4 hours and released at 25 ºC. After 10 min, CBZ was added at 200 µg/ml and cells collected 15 min later. Extracts were immunoprecipitated and analysed as in (A). **(E)** *mad1-GFP* or *mad3-GFP* Δ*dis2 cdc25-22* strains expressing either bub1-6HA or bub1-SATATA-6HA were treated as in (D) and analysed as in (A). (Mw) Molecular weight marker. 5% input of NP-40 yeast extracts (E). Asterisk shows non-specific binding.

Figure S4, related to Figure 4

(A) Log phase cultures of *cdc25-22 bub1-6HA mad2-GFP* cells expressing either *spc7* or *spc7-T12A* were shifted to 35.5 ºC for 4 hours to arrest at G2/M and then released at 25 ºC. After 10 min, CBZ was added at 200 μg/ml and cells were collected 15 min later. NP-40 extracts were immunoprecipitated with rabbit anti-GFP (I) or rabbit serum (PI). Immunoprecipitated material was subsequently analysed by immunoblot using anti-HA and sheep anti-GFP. **(B)** Following incubation for 4 hours at 18 ºC to arrest in mitosis, NP-40 extracts were prepared from *mad3-GFP* strains expressing *nda3-KM311 bub1-6HA*. Extracts were immunoprecipitated with rabbit anti-Mad1 (I) or rabbit serum (PI) and complexes were analysed by immunoblot using anti-HA and rabbit anti-Mad1. (**C)** Log phase *nda3-KM311 bub1-6HA mad3-GFP* strains expressing either *spc7 bub3*$^{+}$ or *spc7-12TA* Δ*bub3* were incubated at 18 ºC for 4 hours. Extracts were immunoprecipitated and analysed as in (A). (Mw) Molecular weight marker. 5% input of NP-40 yeast extracts (E). Asterisk shows non-specific binding.

Supplemental Experimental Procedures

Cell culture and synchronisation

Media, growth and maintenance of strains were as described previously [S1]. Strains used in this study are listed below. YES 10-40% lactose gradients were prepared in a Fisherbrand gradient mixer. Cells in mid log phase were placed on the top and after centrifugation, synchronised early G2 cells were taken from the top of the broad band of cells concentrated at the centre of the gradient. For *cdc25-22* arrest, cells were grown in YES medium overnight at 25 ºC to mid log phase and then shifted to 35.5 ºC for 4 hours. To release, the culture was rapidly cooled to 25 ºC. For mitotic arrests, mid log phase *nda3-KM311* cells growing in YES were arrested at 18 ºC for different durations. Mad2 overexpression assays were made by growing *pREP3x-mad2* strains in minimal glutamate medium supplemented with 5 µg/ml thiamine overnight at 30 ºC. Mid log phase cells were washed twice with the same medium lacking thiamine, and inoculated into fresh media. Cells were then incubated for either 16 or 18 hours at 30 ºC.

Plasmid and strain construction

DNA containing full length *spc7* and ~500 bp 5' promoter and ~200 bp of 3' UTR was cloned into the *SphI* and *BamHI* sites of *pLYS1U* [S2]. Integration at the *lys1* locus was confirmed by PCR. To create mutants of *spc7*, fragments of 1.4 Kb flanked by unique restriction sites *MscI* and *AgeI* were synthesised by GeneArt (Life TechnologiesTM) with the following threonines or serine mutated to alanine T77, S221, T257, T338, T366, T395, T413, T422, T453, T507, T529, T552 (*spc7-12TA*) or T257, T338, T366, T395, T422, T453, T507, T529, T552 (*spc7-9TA*) or T338, T366, T395, T422, T453, T507, T529 (*spc7-7TA*) or T257, T366, T422, T507, T552 (*spc7-5TA*) or T257, T422, T552 (*spc7-3TA*) or T507 (*spc7-1TA*) or with the following threonines mutated to glutamic acid T257, T338, T366, T395, T422, T453, T507, T529, T552 (*spc7-9TE*). These fragments were excised from the GeneArt vector pMA-RQ using *MscI* and *AgeI* and cloned into *pLYS1U-Spc7*. Wild type and mutants were transformed into *spc7::natMX6/spc7*$^{+}$ heterozygous diploid [S3] after digestion with *NotI*. Carboxy-terminal tagging with GFP was performed by two-step PCR-based gene targeting as described previously [S4, S5] using oligos listed below. *bub1-6HA* or *bub1-ΔGLEBS-6HA* expressed at the endogenous locus were created by cutting the plasmid *pBub1-6HA* [S6] with the single *ClaI* site lying within *bub1* sequence. To express an additional copy of *bub1*, the genomic sequence of *bub1* was cloned as a 4 Kb fragment using restriction sites *BamHI* and *KpnI* into *pJK148* [S7]. Plasmids were linearised with *NruI* and integrated into strains with the *leu1.32* auxotrophic marker. Stable integrations at the *leu1* locus were confirmed by PCR. A fragment containing full length *bub3* or *bub3-R201A,K221A* and ~500bp 5' promoter and ~300bp of 3' UTR and a *bub1* fragment containing the specific mutations in S381A, T383A and T386A (called *bub1-SATATA*) was synthesised by GeneArt (Life TechnologiesTM) and excising from the GeneArt vector *pMA-RQ* using *SfiI*. Bub3 fragments were transformed into a *bub3::ura4* strain [S8] or *SalI* or *BssHII* used to clone it into *pLYS1U* or *pLYS1K*. The *bub1* mutant was first cloned as a 2.3 Kb fragment using restriction sites *XhoI* and *SpeI* into *pBSK-bub1*$^{+}$. This Plasmid was then linearised with *BamHI* and *SphI* and transformed into a *bub1::ura4* strain [S6]. Integration of *bub1-SATATA* and *bub3-R201,K221A* at their endogenous loci was selected for on agar plates containing 0.5 mg/ml 5-FOA (Fermentas) and verified by PCR-sequencing. To generate *6HisGST-spc7* and *6HisGST-Spc7-9TE*, a gene fragment encoding Spc7 residues 241-561 was amplified by PCR from *pLYS1U-spc7* or *pLYS1U-Spc7-9TE* plasmids respectively using Gateway Technology (ThermoFisher Scientific).

List of the strains used in this study annotated by initial appearance

Figure 1A
JM8876: *h? bub1-GFP:kanR fta3-mRFP:hygR spc7::natR lys1::spc7:ura4+pREP3x-mad2*
JM8878: *h? bub1-GFP:kanR fta3-mRFP:hygR spc7::natR lys1::spc7-1TA:ura4+pREP3x-mad2*
JM8880: *h? bub1-GFP:kanR fta3-mRFP:hygR spc7::natR lys1::spc7-3TA:ura4+pREP3x-mad2*
JM8882: *h? bub1-GFP:kanR fta3-mRFP:hygR spc7::natR lys1::spc7-5TA:ura4+pREP3x-mad2*
JM8884: *h? bub1-GFP:kanR fta3-mRFP:hygR spc7::natR lys1::spc7-7TA:ura4+pREP3x-mad2*
JM7080: *h? bub1-GFP:kanR fta3-mRFP:hygR spc7::natR lys1::spc7-9TA:ura4+pREP3x-mad2*
JM8888: *h? bub1-GFP:kanR fta3-mRFP:hygR spc7::natR lys1::spc7-12TA:ura4+pREP3x-mad2*

Figure 1B

JM9533: *h? nda3-KM311 plo1-GFP:kanR mad3::ura4*
JM9519: *h? nda3-KM311 plo1-GFP:kanR spc7::natMX6 lys1::spc7:ura4*
JM9522: *h? nda3-KM311 plo1-GFP:kanR spc7::natMX6 lys1::spc7-1TA:ura4*
JM9523: *h? nda3-KM311 plo1-GFP:kanR spc7::natMX6 lys1::spc7-3TA:ura4*
JM9525: *h? nda3-KM311 plo1-GFP:kanR spc7::natMX6 lys1::spc7-5TA:ura4*
JM9527: *h? nda3-KM311 plo1-GFP:kanR spc7::natMX6 lys1::spc7-7TA:ura4*
JM9529: *h? nda3-KM311 plo1-GFP:kanR spc7::natMX6 lys1::spc7-9TA:ura4*
JM9531: *h? nda3-KM311 plo1-GFP:kanR spc7::natMX6 lys1::spc7-12TA:ura4*

Figure 1C

JM7964: *h- nda3-KM311 fta3-mRFP:hygR nsk1-GFP:kanR spc7::natMX6 lys1::spc7:ura4*
JM7969: *h+ nda3-KM311 fta3-mRFP:hygR nsk1-GFP:kanR mad3::ura4*
JM8530: *h? nda3-KM311 fta3-mRFP:hygR nsk1-GFP:kanR spc7::natMX6 lys1::spc7-1TA:ura4*
JM8531: *h? nda3-KM311 fta3-mRFP:hygR nsk1-GFP:kanR spc7::natMX6 lys1::spc7-3TA:ura4*
JM8533: *h? nda3-KM311 fta3-mRFP:hygR nsk1-GFP:kanR spc7::natMX6 lys1::spc7-5TA:ura4*
JM8535: *h? nda3-KM311 fta3-mRFP:hygR nsk1-GFP:kanR spc7::natMX6 lys1::spc7-7TA:ura4*
JM7965: *h+ nda3-KM311 fta3-mRFP:hygR nsk1-GFP:kanR spc7::natMX6 lys1::spc7-9TA:ura4*
JM7967: *h- nda3-KM311 fta3-mRFP:hygR nsk1-GFP:kanR spc7::natMX6 lys1::spc7-12TA:ura4*

Figure 1D

JM7964: *h- nda3-KM311 fta3-mRFP:hygR nsk1-GFP:kanR spc7::natMX6 lys1::spc7:ura4*
JM7967: *h- nda3-KM311 fta3-mRFP:hygR nsk1-GFP:kanR spc7::natMX6 lys1::spc7-12TA:ura4*
JM9293: *h+nda3-KM311 fta3-mRFP:hygR nsk1-GFP:kanR spc7::natMX6 lys1::spc7-12TA:ura4 leu1::bub1*
JM8706: *h- nda3-KM311 fta3-mRFP:hygR nsk1-GFP:kanR spc7::natMX6 lys1::spc7-12TA:ura4 bub3::ura4*
JM9311: *h? nda3-KM311 fta3-mRFP:hygR nsk1-GFP:kanR spc7::natMX6 lys1::spc7-12TA:ura4 his::bub3:kanR*

Figure 2A

JM8891: *h+ sid4-TdTomato:natMX6 bub3-L-GFP:kanR*
JM8893: *h+ sid4-TdTomato:natMX6 bub3-RA,KA-L-GFP:kanR*
JM7375: *h+ nda3-KM311 sid4-TdTomato:natMX6 bub1-GFP:kanR bub3::hygR lys::bub3:ura4*
JM7378: *h- nda3-KM311 sid4-TdTomato:natMX6 bub1-GFP:kanR bub3::hygR lys::bub3-RA, KA:ura4*
JM9134: *h- sid4-TdTomato:hygR bub3-L-GFP:kanR spc7::natMX6 lys1::spc7-9TE:ura4*
JM9136: *h+sid4-TdTomato:hygR bub3-RA,KA-L-GFP:kanR spc7::natMX6 lys1::spc7-9TE:ura4*
JM9166: *h? sid4-TdTomato:hygR bub1-GFP:kanR bub3:hygR spc7::natMX6 lys1::spc7-9TE:ura4*
JM9168: *h? sid4-TdTomato:hygR bub1-GFP:kanR bub3-RA,KA:hygR spc7::natMX6 lys1::spc7-9TE:ura4*

Figure 2B

JM7546: *h- bub1-6HA:ura4 bub3::hygR lys1::bub3-GFP:kanR*
JM7548: *h- bub1-6HA:ura4 bub3::hygR lys1::bub3-RA,KA-GFP:kanR*

Figure 2C

JM7546: *h- bub1-6HA:ura4 bub3::hygR lys1::bub3-GFP:kanR*
JM7548: *h- bub1-6HA:ura4 bub3::hygR lys1::bub3-RA,KA-GFP:kanR*

Figure 2D

JM8097: *h? nda3-KM311 fta3-TdTomato:natMX6 nsk1-GFP:kanR mad3::hygR*
JM8933: *h? nda3-KM311 fta3-TdTomato:natMX6 nsk1-GFP:kanR bub3:hygR*
JM8889: *h? nda3-KM311 fta3-TdTomato:natMX6 nsk1-GFP:kanR bub3-RA,KA:hygR*
JM8935: *h? nda3-KM311 fta3-TdTomato:natMX6 nsk1-GFP:kanR bub3-RA,KA:hygR lys::bub3-RA,KA:ura4*
JM9003: *h? nda3-KM311 fta3-TdTomato:natMX6 nsk1-GFP:kanR bub3-RA,KA:hygR lys::bub3-RA,KA:ura4 bub1(ΔGLEBS) ade6-M210*
JM9662: *h? nda3-KM311 fta3-TdTomato:natMX6 nsk1-GFP:kanR bub3-RA,KA:hygR lys::bub3-RA,KA:ura4 leu1::bub1*

Figure 2E
JM4300: *h+ nda3-KM311*
JM8990: *h- bub3-L-GFP:hygR*
JM9068: *h- bub3-RA,KA-L-GFP:hygR*
JM9104: *h- bub3-RA,KA-L-GFP:hygR lys1::bub3-RA,KA-L-GFP:kanR*

Figure 3A
JM8826: *h+ nda3-KM311 bub1-6HA:ura4*
JM8729: *h? nda3-KM311 mad2-GFP:kanR bub1-6HA:ura4*
JM8733: *h? nda3-KM311 mad3-GFP:kanR bub1-6HA:ura4*

Figure 3B
JM8729: *h? nda3-KM311 mad2-GFP:kanR bub1-6HA:ura4*
JM8733: *h? nda3-KM311 mad3-GFP:kanR bub1-6HA:ura4*

Figure 3C
JM8729: *h? nda3-KM311 mad2-GFP:kanR bub1-6HA:ura4*
JM9399: *h? nda3-KM311 mad2-GFP:kanR bub1-6HA:ura4 dis2::natR*
JM8733: *h? nda3-KM311 mad3-GFP:kanR bub1-6HA:ura4*
JM9374: *h? nda3-KM311 mad3-GFP:kanR bub1-6HA:ura4 dis2::natR*

Figure 3D
JM9392: *h? cdc25-22 bub1-6HA:ura4 mad2-GFP:kanR dis2::natR*
JM9403: *h? cdc25-22 bub1-6HA:ura4 mad2-GFP:kanR dis2::natR mph1::hygR*

Figure 3E
JM9392: *h? cdc25-22 bub1-6HA:ura4 mad2-GFP:kanR dis2::natR*
JM9488: *h? cdc25-22 bub1(SATATA)-6HA:ura4 mad2-GFP:kanR dis2::natR*

Figure 4A
JM8729: *h? nda3-KM311 mad2-GFP:kanR bub1-6HA:ura4*
JM8901: *h+ nda3-KM311 mad2-GFP:kanR bub1-6HA:ura4 bub3::hygR*
JM8733: *h? nda3-KM311 mad3-GFP:kanR bub1-6HA:ura4*
JM8903: *h+ nda3-KM311 mad3-GFP:kanR bub1-6HA:ura4 bub3::hygR*

Figure 4B
JM8729: *h? nda3-KM311 mad2-GFP:kanR bub1-6HA:ura4*
JM8970: *h- nda3-KM311 mad2-GFP:kanR bub1-6HA:ura4 spc7::natMX6 lys1::spc7-12TA:ura4*
JM8733: *h? nda3-KM311 mad3-GFP:kanR bub1-6HA:ura4*
JM8972: *h- nda3-KM311 mad3-GFP:kanR bub1-6HA:ura4 spc7::natMX6 lys1::spc7-12TA:ura4*

Figure 4C
JM8729: *h? nda3-KM311 mad2-GFP:kanR bub1-6HA:ura4*
JM8970: *h- nda3-KM311 mad2-GFP:kanR bub1-6HA:ura4 spc7::natMX6 lys1::spc7-12TA:ura4*
JM9229: *h? nda3-KM311 mad2-GFP:kanR bub1-6HA:ura4 spc7::natMX6 lys1::spc7-12TA:ura4 bub3::hygR*

Supplemental Figure 1B
JM8876: *bub1-GFP:kanR fta3-mRFP:hygR spc7::natR lys1::spc7:ura4+pREP3x-mad2*
JM8878: *bub1-GFP:kanR fta3-mRFP:hygR spc7::natR lys1::spc7-1TA:ura4+pREP3x-mad2*
JM8880: *bub1-GFP:kanR fta3-mRFP:hygR spc7::natR lys1::spc7-3TA:ura4+pREP3x-mad2*
JM8882: *bub1-GFP:kanR fta3-mRFP:hygR spc7::natR lys1::spc7-5TA:ura4+pREP3x-mad2*
JM8884: *bub1-GFP:kanR fta3-mRFP:hygR spc7::natR lys1::spc7-7TA:ura4+pREP3x-mad2*
JM7080: *bub1-GFP:kanR fta3-mRFP:hygR spc7::natR lys1::spc7-9TA:ura4+pREP3x-mad2*
JM8888: *bub1-GFP:kanR fta3-mRFP:hygR spc7::natR lys1::spc7-12TA:ura4+pREP3x-mad2*

Supplemental Figure 1C
JM8876: *bub1-GFP:kanR fta3-mRFP:hygR spc7::natR lys1::spc7:ura4+pREP3x-mad2*
JM8878: *bub1-GFP:kanR fta3-mRFP:hygR spc7::natR lys1::spc7-1TA:ura4+pREP3x-mad2*
JM8880: *bub1-GFP:kanR fta3-mRFP:hygR spc7::natR lys1::spc7-3TA:ura4+pREP3x-mad2*
JM8882: *bub1-GFP:kanR fta3-mRFP:hygR spc7::natR lys1::spc7-5TA:ura4+pREP3x-mad2*
JM8884: *bub1-GFP:kanR fta3-mRFP:hygR spc7::natR lys1::spc7-7TA:ura4+pREP3x-mad2*
JM7080: *bub1-GFP:kanR fta3-mRFP:hygR spc7::natR lys1::spc7-9TA:ura4+pREP3x-mad2*
JM8888: *bub1-GFP:kanR fta3-mRFP:hygR spc7::natR lys1::spc7-12TA:ura4+pREP3x-mad2*
JM9533: *h$^{?}$ nda3-KM311 plo1-GFP:kanR mad3::ura4*
JM9519: *h$^{?}$ nda3-KM311 plo1-GFP:kanR spc7::natMX6 lys1::spc7:ura4*
JM9522: *h$^{?}$ nda3-KM311 plo1-GFP:kanR spc7::natMX6 lys1::spc7-1TA:ura4*
JM9523: *h$^{?}$ nda3-KM311 plo1-GFP:kanR spc7::natMX6 lys1::spc7-3TA:ura4*
JM9525: *h$^{?}$ nda3-KM311 plo1-GFP:kanR spc7::natMX6 lys1::spc7-5TA:ura4*
JM9527: *h$^{?}$ nda3-KM311 plo1-GFP:kanR spc7::natMX6 lys1::spc7-7TA:ura4*
JM9529: *h$^{?}$ nda3-KM311 plo1-GFP:kanR spc7::natMX6 lys1::spc7-9TA:ura4*
JM9531: *h$^{?}$ nda3-KM311 plo1-GFP:kanR spc7::natMX6 lys1::spc7-12TA:ura4*

Supplemental Figure 1D
JM9533: *h$^{?}$ nda3-KM311 plo1-GFP:kanR mad3::ura4*
JM9519: *h$^{?}$ nda3-KM311 plo1-GFP:kanR spc7::natMX6 lys1::spc7:ura4*
JM9527: *h$^{?}$ nda3-KM311 plo1-GFP:kanR spc7::natMX6 lys1::spc7-7TA:ura4*
JM9531: *h$^{?}$ nda3-KM311 plo1-GFP:kanR spc7::natMX6 lys1::spc7-12TA:ura4*

Supplemental Figure 1E
JM8729: *h$^{?}$ nda3-KM311 mad2-GFP:kanR bub1-6HA:ura4*
JM8970: *h^{-} nda3-KM311 mad2-GFP:kanR bub1-6HA:ura4 spc7::natMX6 lys1::spc7-12TA:ura4*

Supplemental Figure 1F
JM8729: *h$^{?}$ nda3-KM311 mad2-GFP:kanR bub1-6HA:ura4*
JM8901: *h^{+}nda3-KM311 mad2-GFP:kanR bub1-6HA:ura4 bub3::hygR*
JM8741: *h$^{?}$ nda3-KM311 mad2-GFP:kanR bub1(ΔGLEBS)-6HA:ura4*

Supplemental Figure 1G
JM7969: *h^{+} nda3-KM311 fta3-mRFP:hygR nsk1-GFP:kanR mad3::ura4*
JM7964: *h^{-} nda3-KM311 fta3-mRFP:hygR nsk1-GFP:kanR spc7::natMX6 lys1::spc7:ura4*

Supplemental Figure 1H
JM7964: *h^{-} nda3-KM311 fta3-mRFP:hygR nsk1-GFP:kanR spc7::natMX6 lys1::spc7:ura4*
JM7967: *h^{-} nda3-KM311 fta3-mRFP:hygR nsk1-GFP:kanR spc7::natMX6 lys1::spc7-12TA:ura4*
JM8690: *h^{-} nda3-KM311 fta3-mRFP:hygR nsk1-GFP:kanR spc7::natMX6 lys1::spc7:ura4 bub1(ΔGLEBS) ade6-210*
JM8698: *h^{-} nda3-KM311 fta3-mRFP:hygR nsk1-GFP:kanR spc7::natMX6 lys1::spc7-12TA:ura4 bub1(ΔGLEBS) ade6-210*
JM8700: *h^{-} nda3-KM311 fta3-mRFP:hygR nsk1-GFP:kanR spc7::natMX6 lys1::spc7:ura4 bub3::ura4*
JM8706: *h^{-} nda3-KM311 fta3-mRFP:hygR nsk1-GFP:kanR spc7::natMX6 lys1::spc7-12TA:ura4 bub3::ura4*

Supplemental Figure 2B
JM8097: *h$^{?}$ nda3-KM311 fta3-TdTomato:natMX6 nsk1-GFP:kanR mad3::hygR*
JM8935: *h$^{?}$ nda3-KM311 fta3-TdTomato:natMX6 nsk1-GFP:kanR bub3-RA,KA:hygR lys::bub3-RA,KA:ura4*
JM8107: *h$^{?}$ nda3-KM311 fta3-TdTomato:natMX6 nsk1-GFP:kanR bub3::hygR lys1::bub3-RA, KA:ura4*
JM9660: *h$^{?}$ nda3-KM311 fta3-TdTomato:natMX6 nsk1-GFP:kanR bub3-RA,KA:hygR leu1::bub1*
JM9667: *h$^{?}$ nda3-KM311 fta3-TdTomato:natMX6 nsk1-GFP:kanR bub3:hygR leu1::bub1*
JM9668: *h$^{?}$ nda3-KM311 fta3-TdTomato:natMX6 nsk1-GFP:kanR bub3:hygR lys::bub3:ura4 leu1::bub1*

Supplemental Figure 3A
JM8725: *h$^{?}$ nda3-KM311 mad1-GFP:kanR bub1-6HA:ura4*

JM8729: *h? nda3-KM311 mad2-GFP:kanR bub1-6HA:ura4*
JM8733: *h? nda3-KM311 mad3-GFP:kanR bub1-6HA:ura4*

Supplemental Figure 3B
JM8725: *h? nda3-KM311 mad1-GFP:kanR bub1-6HA:ura4*
JM9452: *h+ nda3-KM311 mad1-GFP:kanR bub1-6HA:ura4 dis2::natR*
JM9399: *h? nda3-KM311 mad2-GFP:kanR bub1-6HA:ura4 dis2::natR*
JM9374: *h? nda3-KM311 mad3-GFP:kanR bub1-6HA:ura4 dis2::natR*

Supplemental Figure 3C
JM4267: *h+ cdc25-22 sid4-tdtomato:natMX6 nsk1-gfp:KanR*
JM9231: *h+ cdc25-22 sid4-tdtomato:natMX6 nsk1-gfp:KanR mad3::hygR*
JM9116: *h? cdc25-22 nsk1-gfp:KanR spc7::natMX6 lys1::spc7(T12A):ura4*

Supplemental Figure 3D
JM8978: *h? cdc25-22 bub1-6HA:ura4 mad2-GFP:kanR*
JM9319: *h+ cdc25-22 bub1-6HA:ura4 mad2-GFP:kanR mph1::hygR*

Supplemental Figure 3E
JM9455: *h- cdc25-22 mad1-GFP:kanR bub1-6HA:ura4 dis2::natR*
JM9465: *h? cdc25-22 mad1-GFP:kanR bub1(SATATA)-6HA:ura4 dis2::natR*
JM9376: *h? cdc25-22 mad3-GFP:kanR bub1-6HA:ura4 dis2::natR*
JM9479: *h? cdc25-22 mad3-GFP:kanR bub1(SATATA)-6HA:ura4 dis2::natR*

Supplemental Figure 4A
JM8978: *h? cdc25-22 mad2-GFP:kanR bub1-6HA:ura4*
JM9083: *h- cdc25-22 mad2-GFP:kanR bub1-6HA:ura4 spc7::natMX6 lys1::spc7-12TA:ura4*

Supplemental Figure 4B
JM8733: *h? nda3-KM311 mad3-GFP:kanR bub1-6HA:ura4*
JM8972: *h- nda3-KM311 mad3-GFP:kanR bub1-6HA:ura4 spc7::natMX6 lys1::spc7-12TA:ura4*
JM9219: *h? nda3-KM311 mad3-GFP:kanR bub1-6HA:ura4 spc7::natMX6 lys1::spc7-12TA:ura4 bub3::hygR*

Supplemental Figure 4C
JM8733: *h? nda3-KM311 mad3-GFP:kanR bub1-6HA:ura4*
JM9219: *h? nda3-KM311 mad3-GFP:kanR bub1-6HA:ura4 spc7::natMX6 lys1::spc7-12TA:ura4 bub3::hygR*

List of oligonucleotides used in this study

Construction of pLYSU-Spc7
SphI FW
5'TTTATA*GCATGC*TTCTTACAACCGCACATT 3'
BamHI
5'TTTATA*GGATCC*GCGCATTACGGGTTTAACA 3'

Construction of pJK148-bub1
BamHI FW
5'CGCGGATCCCTACAACCTGTTTTTCGCTCATATTCG 3'
KpnI RV
5'CGCGGTACCGTTGTTTAGGAAAGAAAAACTAACCCCAATAAA 3'

C-terminal GFP-tagging of *mad3* and *bub3* alleles
mad3w
5'GATGGCCAACCTGGGACCTGGC3'

mad3x
5’TCCAGTGAAAAGTTCTTCTCCTTTACTCATGAATTCGATATCAAGCTTATCGATACCGTCGACTTC
TTTCGATACTTCCTCATC3’
mad3y
5’GTTTAAACGAGCTCGAATTCATCGATATTAGATTAACAACTATTGT3’
mad3z
5’TATAGAGGTGTAATTACTTATC3’

bub3w
5’CGACCTAAAATTTCATCCGATTCATCA3’
bub3x
5’GGGGATCCGTCGACCTGCAGCGTACGACATGAATTCGATATCAAGCTTATCGATACCGTCGACTG
ACTTTAACTTTGGAGCTGCAAAGTTGGATTC3’
bub3y
5’GTTTAAACGAGCTCGAATTCATCGATAATCGCTCATCAAAAAGCTTCATCCATGTA3’
bub3z
5’CCAAATAGTGTCACATTGTTTTTATATTAAGTA3’

Gateway cloning for expression of Spc7 fusion proteins
attB FW
5’GGGGACAAGTTTGTACAAAAAAGCAGGCTTCGCCACGAGAGAGCAGGTTAATGAT3’
attB RV
5’GGGGACCACTTTGTACAAGAAAGCTGGGTCTTAGTTTCCACGGATTTGAAAAGCCAC3’

Fixed cell fluorescence microscopy

Cells were fixed in 3.7 % formaldehyde for 10 min and mounted in Vectashield mounting medium containing DAPI. Fluorescence imaging of cells expressing GFP, RFP or TdTomato tagged proteins was performed on a Nikon TE-2000 inverted microscope with a 100x 1.49 N.A. objective lens equipped with a Photometrics Coolsnap-HQ2 liquid cooled CCD camera (Photometrics, Tucson, AZ). Images were collected and analysed using Metamorph (version 7.5.9.0 MAG Biosystems Software). Exposure times of 1 second were used for GFP, RFP and TdTomato and 0.25 seconds for DAPI (shown in blue in all images). Stacks of 18 z-sections (0.2µm apart) were taken and projected images were made followed by intensity adjustments. Experiments were conducted at least three times and the mean value presented, more than 250 cells were counted in each repeat.

Protein quantification

bub1-GFP fta3-RFP pREP3x-mad2 cells expressing various *spc7* mutant alleles or wild type *spc7* were grown to mid-log phase in the presence of thiamine and then arrested in metaphase by growing in the absence of thiamine for 18 hours. Following fixation, Bub1-GFP levels were measured in individual cells both at kinetochores *via* colocalisation with Fta3-RFP and in the nucleoplasm. In each case background levels of cellular fluorescence were first removed and for kinetochore-bound Bub1-GFP signal was normalised against background-subtracted Fta3-RFP levels. Average signal intensity measurements in a 10 pixel diameter circle ($0.32\mu m^2$) localised at the maximal intensity of the RFP signal were calculated using MetaMorph (version 7.5.9.0 MAG Biosystems Software). Measurements were taken over three experiments and the individual profiles plotted. Cumulative distributions were generated using R [S9, S10]. Quantification of protein levels across multiple immunoblots was conducted with ImageJ (Gel Analyzer) and distribution of signal between experiments represented with standard deviation throughout. Quantification was performed in the linear range as determined *via* serial exposure intensity analysis. Tat1 (anti-Tubulin) was used to normalise signal intensities were possible.

Single cell analysis of checkpoint maintenance

Cells were grown in YEA medium at 30°C and mounted in # 1.5 glass-bottom culture dishes (Ibidi) that had been coated with 100 µg/ml lectin (Sigma, L1395). Imaging was performed on a DeltaVision Core system (Applied Precision/GE Healthcare) equipped with a climate chamber (set to 16°C). Cells were incubated on the microscope stage at 16°C for 1.5 hours before recording. Pictures were taken with a CoolSnap HQ camera using

a 60x/1.4 Plan Apo oil objective (Olympus) and the 'optical axis integration' algorithm of the SoftWorx software (Applied Precision/GE Healthcare). All images were deconvolved using SoftWorx software. The time of appearance and disappearance of Plo1-GFP at spindle pole bodies was determined by a custom MATLAB (MathWorks) script. The custom MATLAB (MathWorks) script is applied to images of single cells and first determines the maximum intensity within a region of interest, smoothed over five time points. The first and second derivative are used to detect the first strong increase in signal as well as the last strong decrease in signal. The Plo1-GFP maximum intensity before and after these time points is considered the 'baseline'. Additional parameters are used to ensure that the baseline intensities at the start of the increase and at the end of the decrease are in the same range - unless in cells where Plo1-GFP has not delocalised by the end of image acquisition. The time point where Plo1-GFP intensity increases above or decreases below 1.3x the baseline are taken as start and stop to determine the time in mitosis. The automatically detected values are displayed to the user and can be corrected manually, if necessary. Kymographs were assembled using a custom MATLAB (MathWorks) script. Cells that died during mitosis were removed from the analysis.

***in vitro* binding assay**

Expression of fusion proteins was induced in *Escherichia coli BL21 DE3 plysS* cells by incubation with 1mM isopropyl-β-D-thiogalactoside (IPTG) for 3.5 hours at 37ºC. Cells were lysed in ice cold lysis buffer containing 150 mM NaCl, 1 % NP40, 10 mM TrisCl pH 8, 10 % glycerol, 1 mM DTT, 1 mM PMSF and Complete mini EDTA-free Protease Inhibitor Cocktail Tablets (Roche Applied Science) followed by sonication with 20 sec pulse for six cycles (Sonics, Vibra-Cell). Fusion proteins were purified from bacterial lysates *via* their affinity to glutathione-Sepharose beads for 30 min (GE Healthcare). For the *in vitro* assay, yeast lysates (5 mg) were incubated with 6HisGST-Spc7 or 6HisGST-Spc7-9TE bound to Sepharose beads for 2 hours. Beads were washed six times with lysis buffer and proteins were eluted by the addition of SDS-sample buffer heated at 95 ºC for 5 min.

Immunoblot analysis

Cell lysates were prepared by lysing cells in NP40 buffer (1 % NP40, 10 mM TrisCl pH 7.5, 150 mM NaCl, 10 % glycerol) containing 1 mM PMSF, Complete mini EDTA-free Protease Inhibitor Cocktail and Phosphatase Inhibitor Tablets (Roche Applied Science). Concentration was determined using a Bradford assay. Proteins were separated by SDS-polyacrylamide gel electrophoresis (SDS-PAGE), transferred to nitrocellulose membranes and probed with the following antibodies: anti-HA peroxidase rat antibody (Roche Applied Science), mouse anti-Tat1 antibody (a gift from Keith Gull), sheep anti-GFP antibody (a gift from Kevin Hardwick), rabbit anti-Mad1 antibody [S11]. Proteins were visualized using the enhanced chemiluminescence (ECL) detection system according to the manufacturer's instructions (GE Healthcare). In all cases statistics are derived from at least three independent experiments.

Co-immunoprecipitation

Yeast extracts (2 mg) were incubated with normal rabbit serum for 30 min and subsequently with protein A-Sepharose beads (GE Healthcare) for 45 min at 4 ºC. After centrifugation, beads were kept as pre-immune (*PI*) and the same extract was incubated with polyclonal anti-GFP (Immune systems) or rabbit anti-Mad1 antibody [S11] for 2 hours followed by an incubation with protein A-Sepharose beads for another 45 min and the beads were kept as immune (*I*). Beads were washed six times with NP40 buffer and bound proteins were solubilised by the addition of SDS-sample buffer heated at 95 ºC for 5 min.

Supplemental References

S1. Moreno, S., Klar, A., and Nurse, P. (1991). Molecular genetic analysis of fission yeast Schizosaccharomyces pombe. Methods Enzymol *194*, 795-823.

S2. Matsuyama, A., Shirai, A., and Yoshida, M. (2008). A novel series of vectors for chromosomal integration in fission yeast. Biochem Biophys Res Commun *374*, 315-319.

S3. Meadows, J.C., Shepperd, L.A., Vanoosthuyse, V., Lancaster, T.C., Sochaj, A.M., Buttrick, G.J., Hardwick, K.G., and Millar, J.B. (2011). Spindle checkpoint silencing requires association of PP1 to both Spc7 and kinesin-8 motors. Dev Cell *20*, 739-750.

S4. Bahler, J., Wu, J.Q., Longtine, M.S., Shah, N.G., McKenzie, A., 3rd, Steever, A.B., Wach, A., Philippsen, P., and Pringle, J.R. (1998). Heterologous modules for efficient and versatile PCR-based gene targeting in Schizosaccharomyces pombe. Yeast *14*, 943-951.

S5. Krawchuk, M.D., and Wahls, W.P. (1999). High-efficiency gene targeting in Schizosaccharomyces pombe using a modular, PCR-based approach with long tracts of flanking homology. Yeast *15*, 1419-1427.

S6. Bernard, P., Hardwick, K., and Javerzat, J.P. (1998). Fission yeast bub1 is a mitotic centromere protein essential for the spindle checkpoint and the preservation of correct ploidy through mitosis. J Cell Biol *143*, 1775-1787.

S7. Keeney, J.B., and Boeke, J.D. (1994). Efficient targeted integration at leu1-32 and ura4-294 in Schizosaccharomyces pombe. Genetics *136*, 849-856.

S8. Vanoosthuyse, V., Meadows, J.C., van der Sar, S.J., Millar, J.B., and Hardwick, K.G. (2009). Bub3p facilitates spindle checkpoint silencing in fission yeast. Mol Biol Cell *20*, 5096-5105.

S9. R Core Team (2016). R: A language and environment for statistical computing.

S10. Wickham, H. (2009). ggplot2: Elegant Graphics for Data Analysis, (Springer-Verlag New York).

S11. Heinrich, S., Sewart, K., Windecker, H., Langegger, M., Schmidt, N., Hustedt, N., and Hauf, S. (2014). Mad1 contribution to spindle assembly checkpoint signalling goes beyond presenting Mad2 at kinetochores. EMBO Rep *15*, 291-298.